LA-UR- 08-6300

Approved for public release; distribution is unlimited.

Title: ~~High Energy~~ Proton Radiography

Author(s): Merrill, Frank

Intended for: GSI LANL pRad Collaboration Meeting; Darmstadt, Germany

Los Alamos
NATIONAL LABORATORY
EST. 1943

Los Alamos National Laboratory, an affirmative action/equal opportunity employer, is operated by the Los Alamos National Security, LLC for the National Nuclear Security Administration of the U.S. Department of Energy under contract DE-AC52-06NA25396. By acceptance of this article, the publisher recognizes that the U.S. Government retains a nonexclusive, royalty-free license to publish or reproduce the published form of this contribution, or to allow others to do so, for U.S. Government purposes. Los Alamos National Laboratory requests that the publisher identify this article as work performed under the auspices of the U.S. Department of Energy. Los Alamos National Laboratory strongly supports academic freedom and a researcher's right to publish; as an institution, however, the Laboratory does not endorse the viewpoint of a publication or guarantee its technical correctness.

Form 836 (7/06)

Proton Radiography

Frank Merrill

Los Alamos National Laboratory has used high energy protons as a probe in flash radiography for a decade. In this time the proton radiography project has used 800 MeV protons, provided by the LANSCE accelerator facility at LANL, to diagnose over two-hundred dynamic experiments in support of national and international weapons science and stockpile stewardship programs. In addition, 24 GeV protons, provided by the Alternating Gradient Synchrotron at Brookhaven National Laboratory, have been used to study the capability of proton radiography at higher beam energies. Through this effort significant experience has been gained in using proton radiography as a technique to diagnose explosively driven systems. The results of this experience will be presented by relating the spatial, temporal and density resolution performance to the parameters of the incident beam, imaging lens and detectors.

Proton Radiography

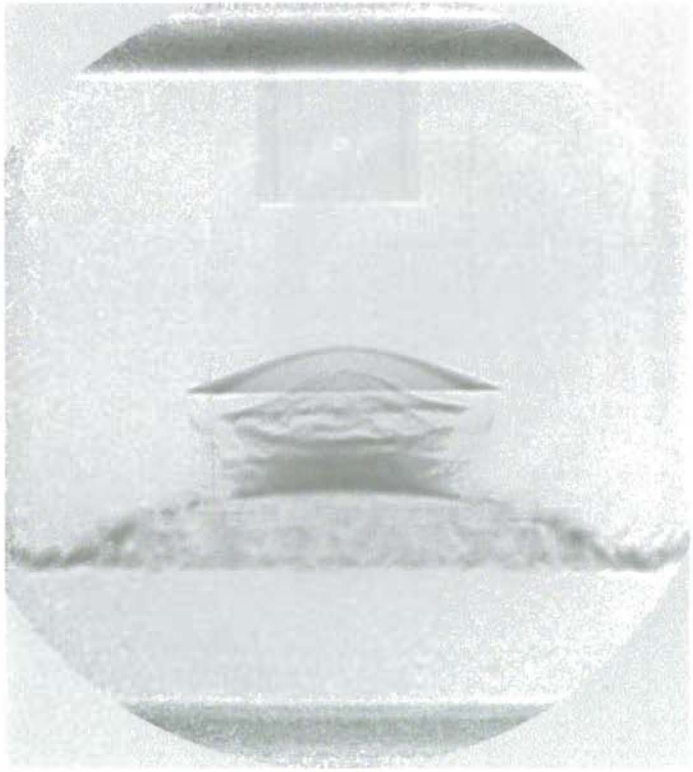

Frank Merrill, LANL
and the pRad collaboration

pRad Collaboration

Bechtel Nevada

Stuart Baker, Alfred Meidinger, Richard Thompson, Josh Tybo

DE-2

Robert Hixson, Paulo Rigg, Darcie Dennis-Kohler

HX-3

Joe Bainbridge, Stephen Dennison, Eric Ferm, Robert Lopez, Mark Marr-Lyon, Carlos Montoya, Paul Rightley Wendy McNeil

LANSCE-1

Andrew Jason, Barbara Blind, Charles Mottershead

LANSCE-6

Leo Bittecker, Rodney McCrady, Chandra Pillai

P-23

William Buttler, David D. Clark, David Holtkamp, Nick King, Kris Kwiatkowski, Kevin Morley, Russ Olson, Paul Nedrow

P-25

Jeffrey Bacon, Bethany Brooks, Camilo Espinoza, Gary Hogan, Brian Hollander, Julian Lopez, Fesseha Mariam, Frank Merrill, Christopher Morris, Matthew Murray, Alexander Saunders, Richard Schirato, Larry Schultz, Cynthia Schwartz, Dale Tupa

S-7

Rodger Liljestrand

X-4

Langdon Bennett, John David Becker, Maria Rightley, Stephen Sterbenz

Proton Interactions

Proton Radiography

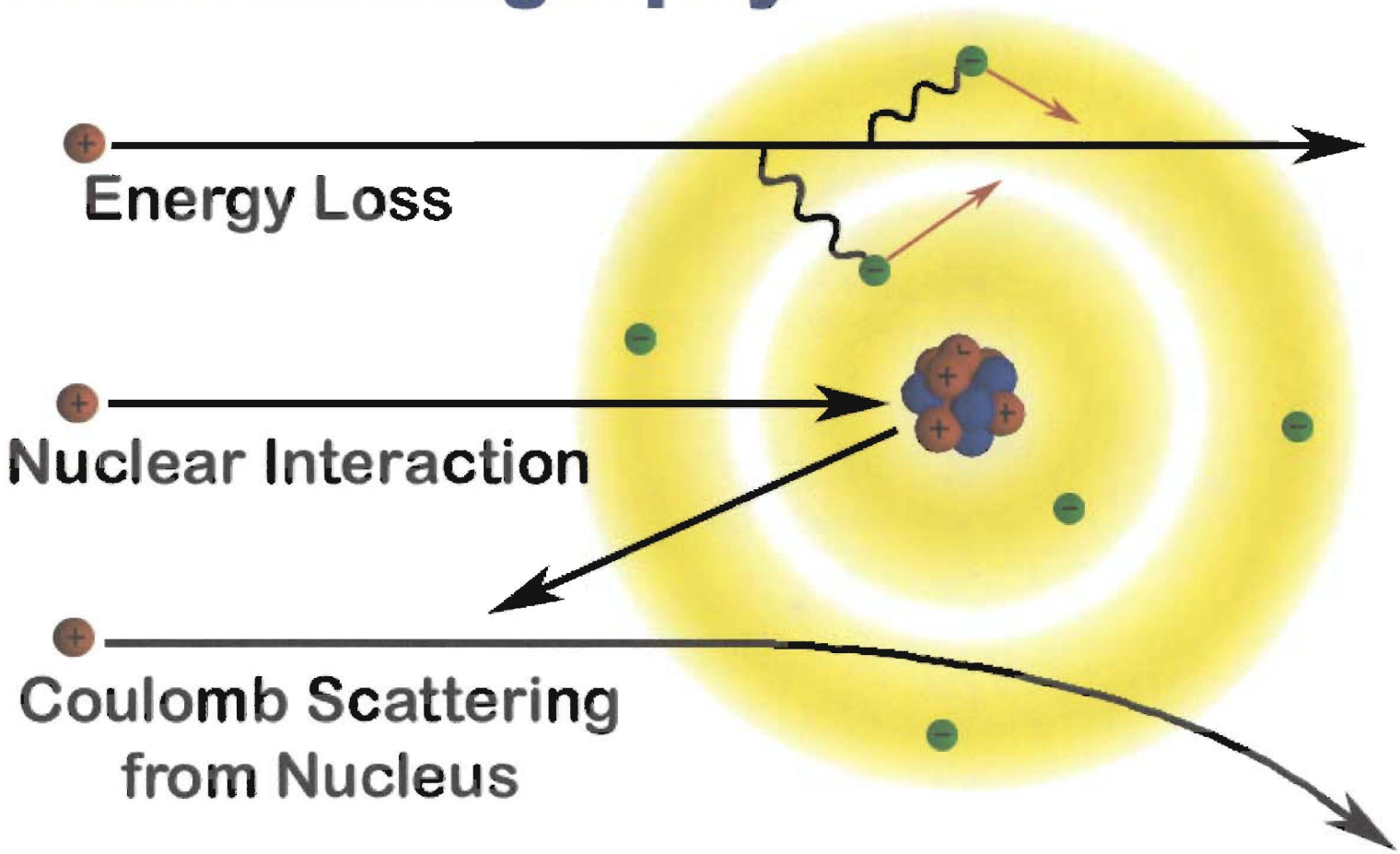

Early Proton Radiography

A. M. Koehler, et al. *Science* **160**, 303 (1968)

Fig. 1. Proton radiograph of aluminum absorber 7 cm in diameter and 18 g/cm² thick, with an additional thickness of 0.035-g/cm² aluminum foil, cut in the shape of a pennant, inserted at a depth of 9 g/cm². The addition of 0.2 percent to the total thickness produces a substantially darker area on the film.

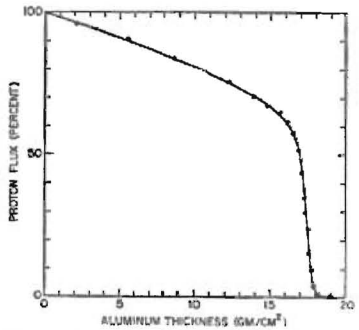

Fig. 2. Proton flux as a function of depth in aluminum. The steeply falling portion of the curve near 18 g/cm² is used to obtain the high contrast of Fig. 1.

J. A. Cookson Naturwissenschaften 61, 184—191 (1974)

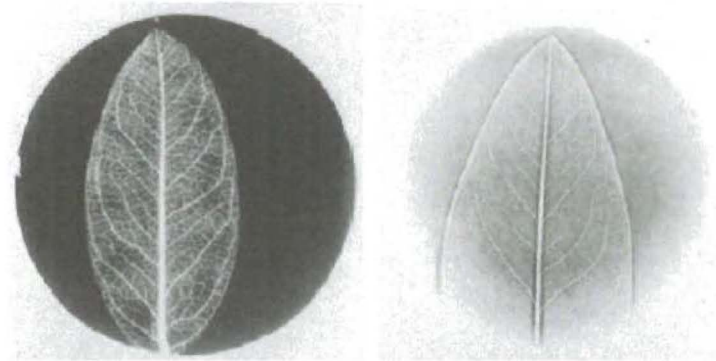

Fig. 6a and b. Radiographs of leaves by a) marginal range radiography with 196 mg/cm² of extra Al absorber, and b) scattering radiography with leaf sandwiched between two 6.9 mg/cm² Al layers and 14 mm from the film

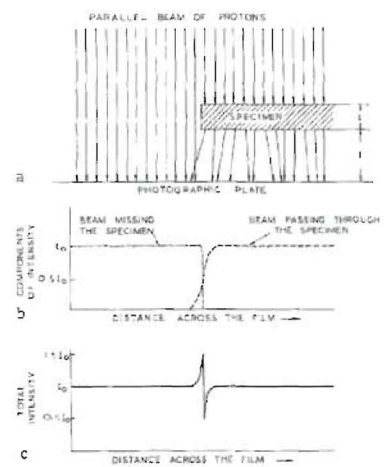

Fig. 7. Illustration of how multiple scattering produces its characteristic edge pattern

Marginal Range Radiography

- Reduce proton beam energy to near end of range.
- Use steep portion of transmission curve to enhance sensitivity to areal density variations.
- Coulomb scattering at low energy results in poor resolution >1.5 mm.
- Contrast generated through proton absorption.

Scattering Radiography

- Edge detection only
- Limited to thin objects
- Contrast generated through position dependent scattering

LANL Transmission Radiography (1995)

188 MeV secondary proton beamline at LANSCE

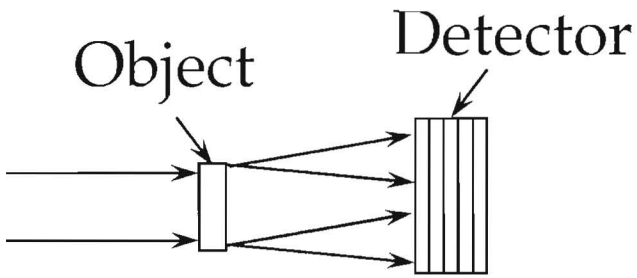

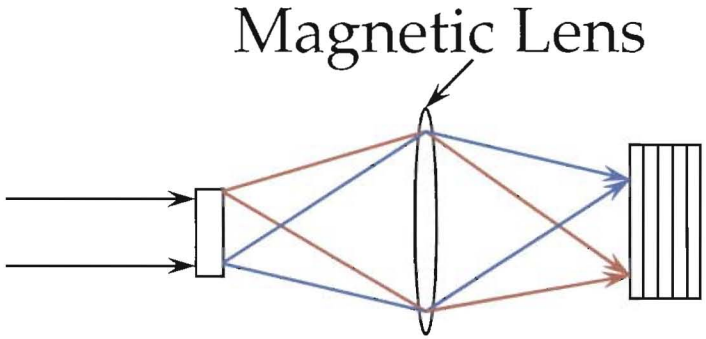

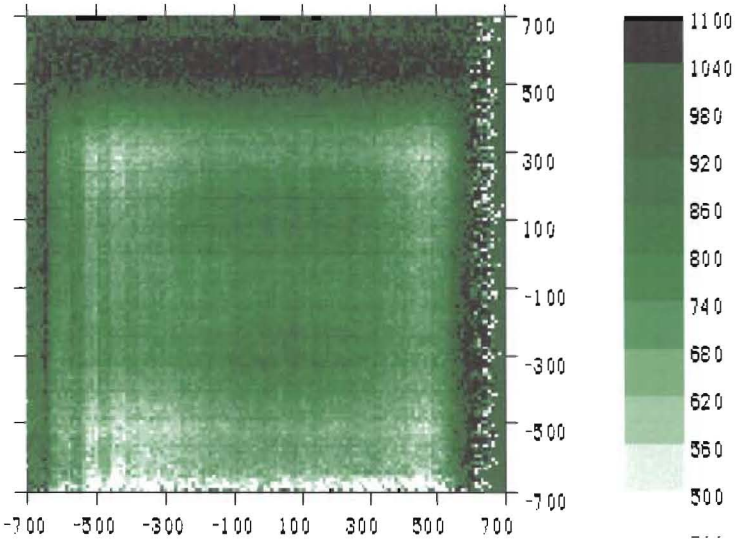

Image at the detector is substantially blurred.

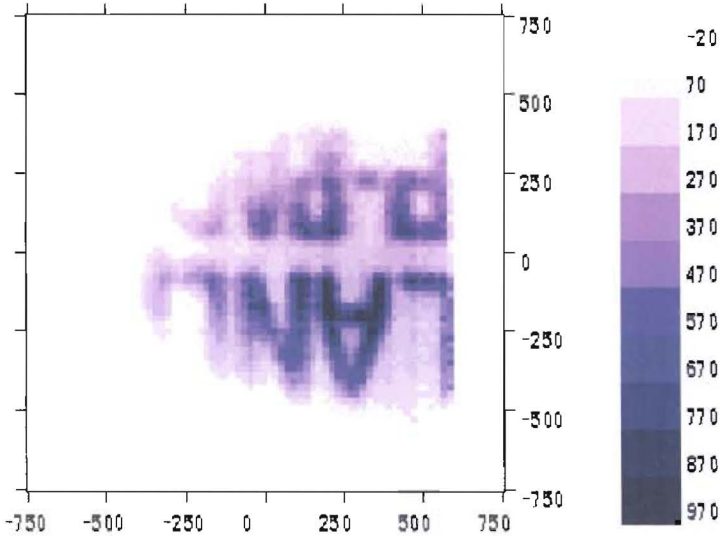

Magnetic imaging lens preserves image with high resolution.

Magnetic Imaging Lens

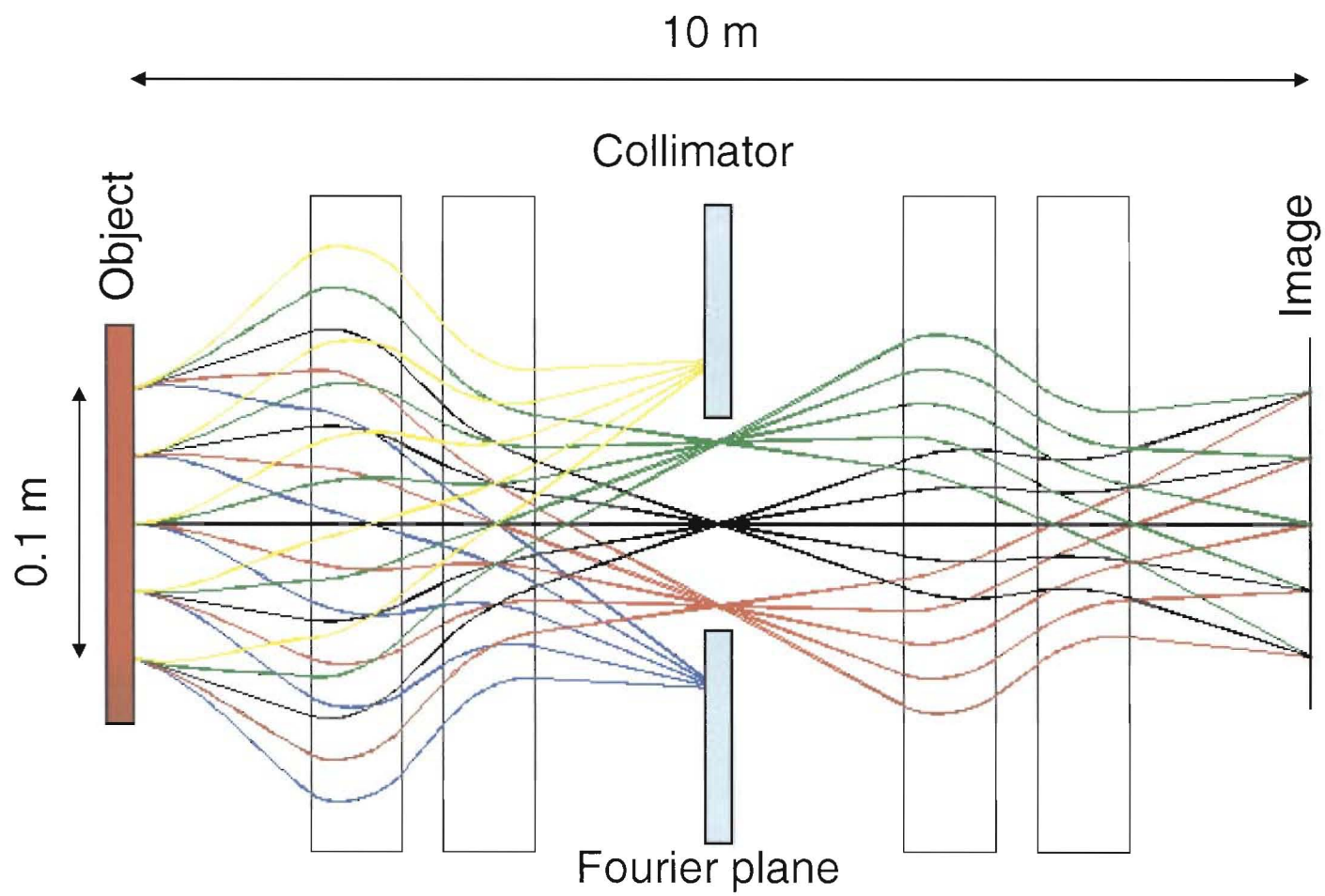

Quadrupole Identity Lens

Contrast from Multiple Coulomb Scattering

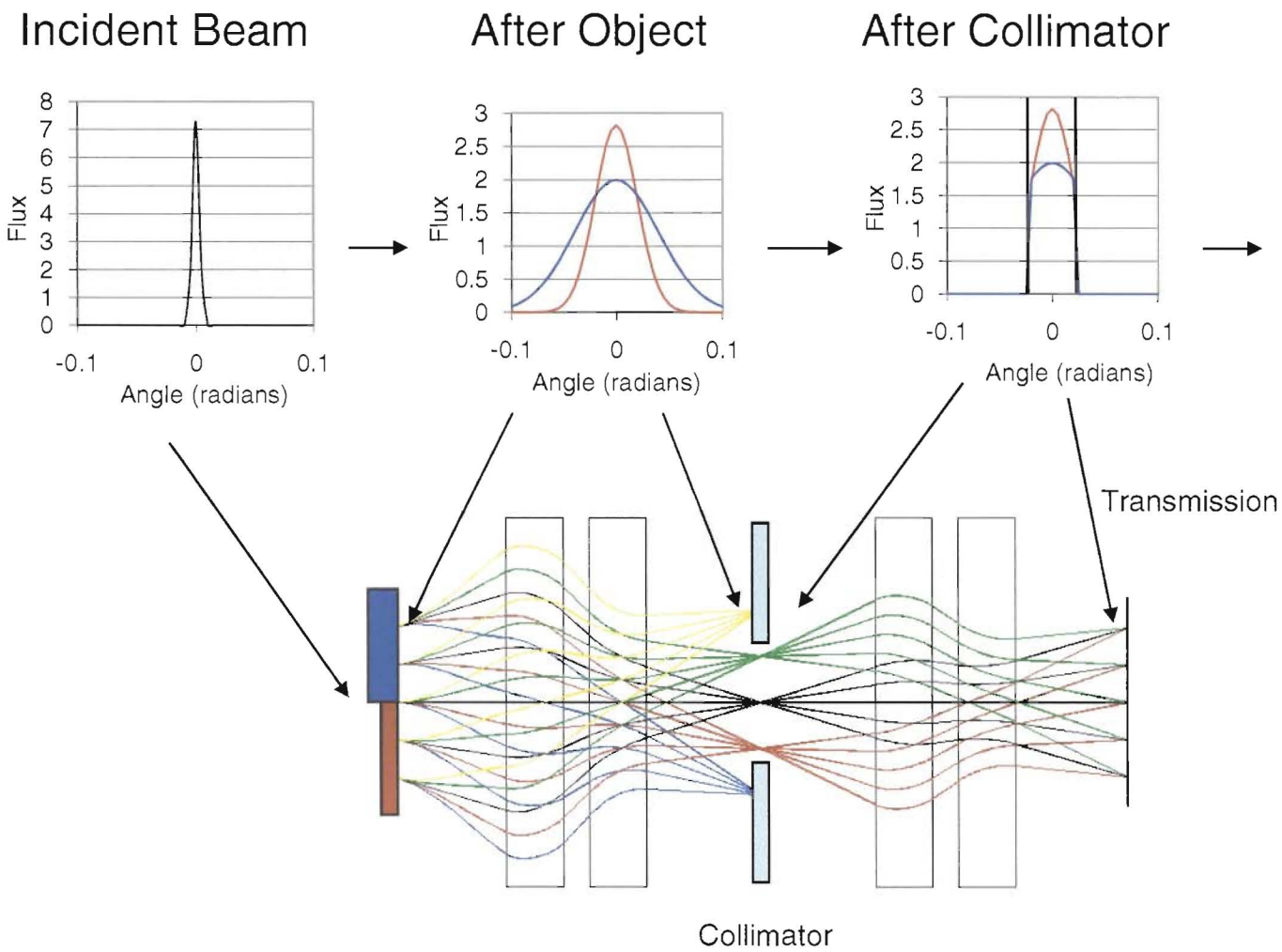

Measured transmission provides information of object thickness

LANSCE Experimental Areas

- Lujan Center
  - ***National security research***
  - ***Materials, bio-science, and nuclear physics***
  - ***National user facility***
- WNR
  - ***National security research***
  - ***Nuclear Physics***
  - ***Neutron Irradiation***
- Proton Radiography
  - ***National security research***
  - ***Dynamic Materials science,***
  - ***Hydrodynamics***
- Isotope Production Facility
  - ***Medical radioisotopes***

800 MeV pRad Facility at LANSCE

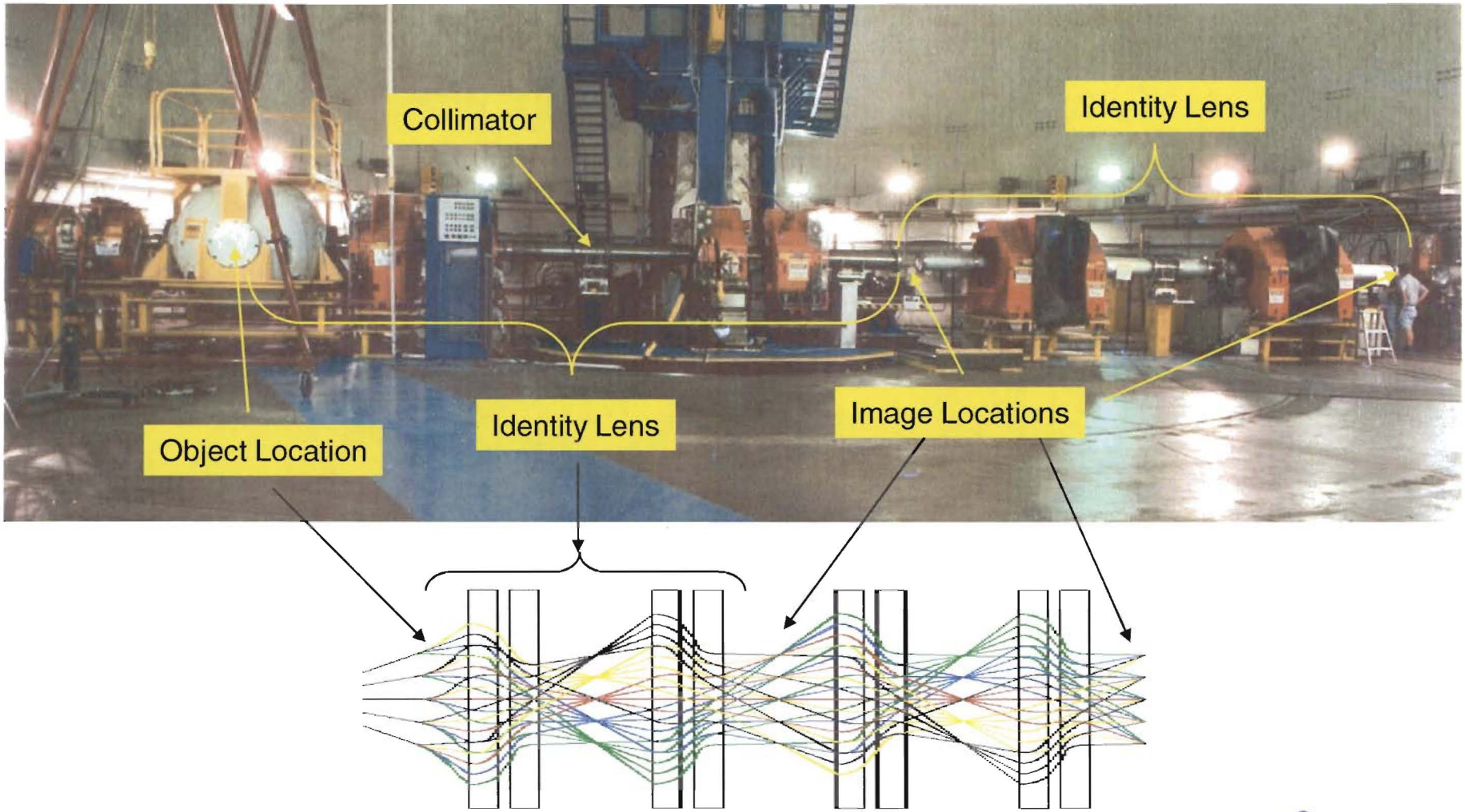

Sensitivity with 800 MeV Protons

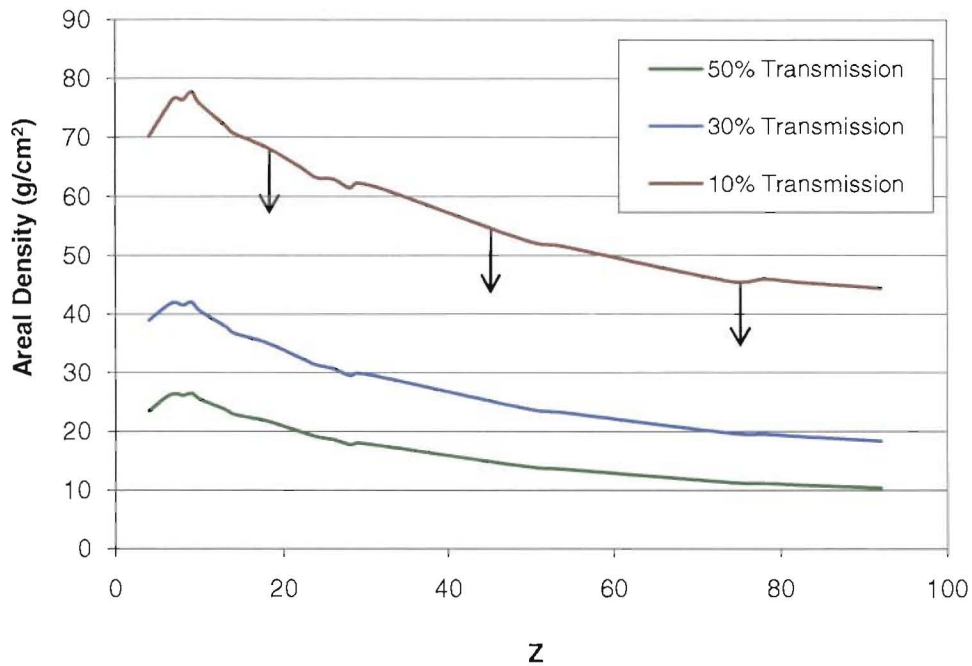

Areal density contours of constant transmission as a function of atomic number.

10% is near the lower limit of reasonable transmission.

- Perform experiments less than ~50 g/cm^2 with 800 MeV proton Radiography

Temporal Resolution

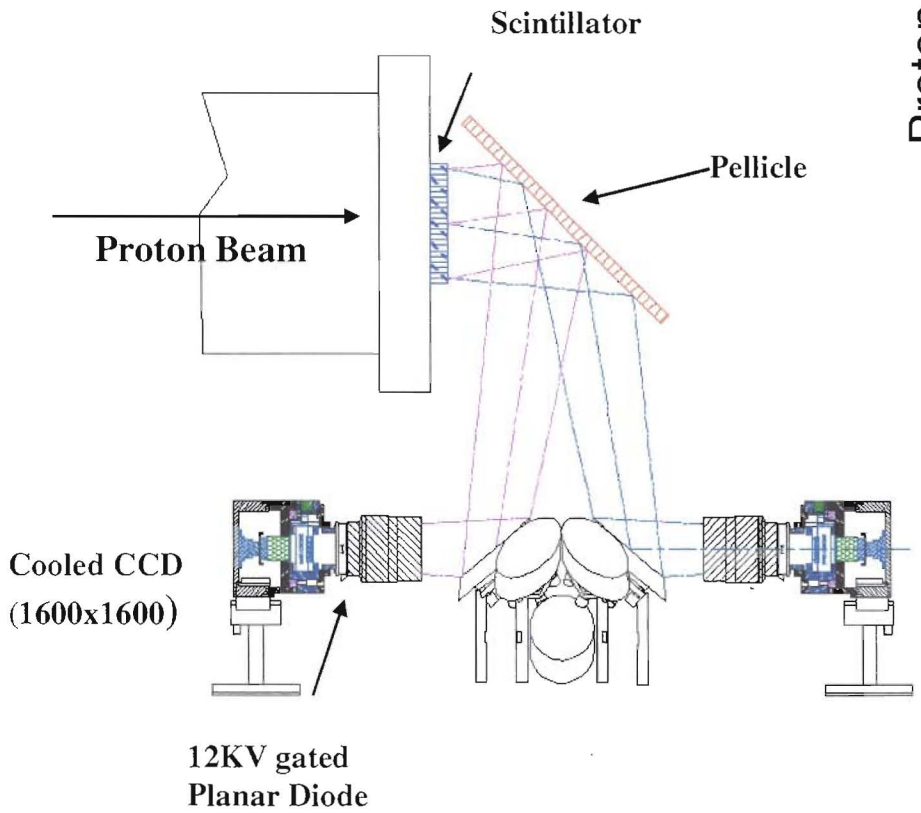

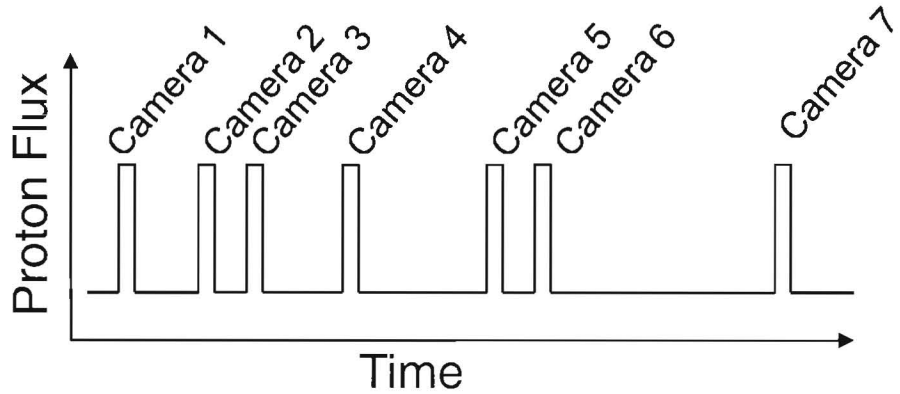

- 15 images at first station
- 22 images at second station
- Typically 100 ns exposure times

Correcting Second Order Chromatic Aberrations

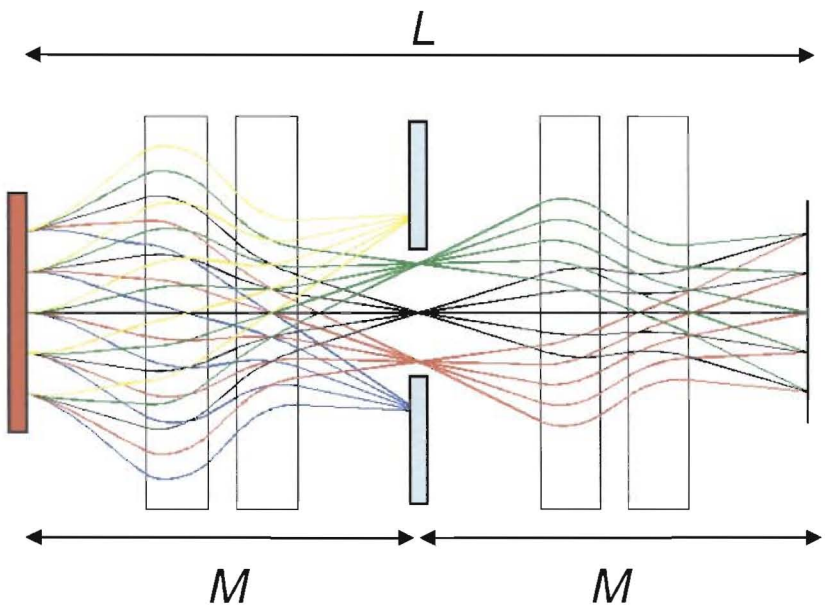

x_o, x_o' - position and angle at object
x_{fp} - position at midpoint of lens
x_i - position and angle at image
δ - $\Delta p/p$
M - Transport matrix for doublet
L - First order Transport matrix
T - Second order Transport tensor

$$L = M^2 = -I$$

Form identity lens from identical doublets

Fourier Plane

$$x_{fp} = M_{11}x_o + M_{12}x_o'$$

$$x_o' = wx_o + \phi$$

$$x_{fp} = M_{11}x_o + M_{12}(wx_o + \phi)$$

$$w = -M_{11}/M_{12}$$

$$x_{fp} = M_{12}\phi$$

Inject beam with position-angle correlation to form Fourier plane at center of lens.

Resolution

$$x_i = L_{11}x_o + L_{12}x_o' + T_{116}x_o\delta + T_{126}x_o'\delta$$

$$x_i = -x_o + T_{116}x_o\delta + T_{126}(wx_o + \phi)\delta$$

$$w = -T_{116}/T_{126} = -M_{11}/M_{12} \quad *$$

$$w = -M_{11}/M_{12}$$

$$\Delta x_i = T_{126}\phi\delta$$

Dominates Blur

Same position-angle correlation which forms a Fourier plane at the center of the lens also cancels second order chromatic terms.

* C.T. Mottershead and J. D. Zumbro, "Magnetic Optics for Proton Radiography", Proceedings of the 1997 Particle Accelerator Conference

Areal Density Reconstruction

$$T_{nuclear} = e^{-x/\lambda}$$

Nuclear removal processes

$$T_{MCS} = 1 - e^{-\theta_c^2 / 2\theta_o^2}$$

$$\theta_o = \frac{14.1 MeV}{p\beta}\sqrt{\frac{x}{x_o}}$$

Multiple Coulomb Scattering with collimation:

ϑ_o - scattering angle (radians)
x - areal density
x_o - radiation length
p - momentum (MeV)
β - relativistic velocity

$$T = e^{-x/\lambda}\left(1 - e^{-\left(\frac{\theta_c p\beta}{14.1 MeV}\right)^2 \frac{x_o}{2x}}\right)$$

Total Transmission
- inverted to determine areal density, x

Radiographic Analysis

"Raw" Radiograph

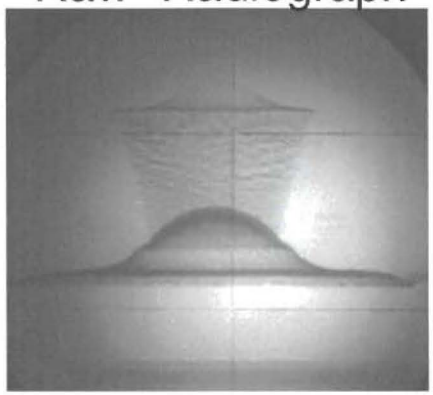

-

Dark Field

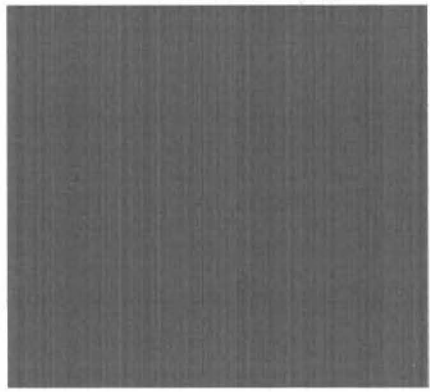

=

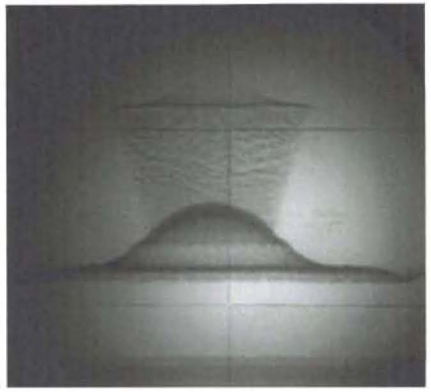

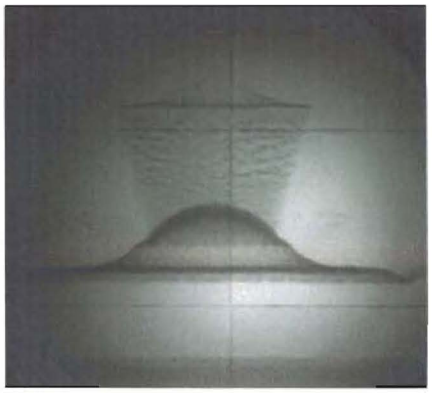

÷

Beam Picture

=

Transmission

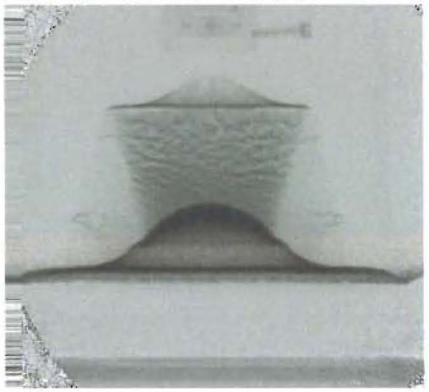

Density Reconstruction

Invert to calculate Areal Density

$$T = e^{-x/\lambda}\left(1 - e^{-\left(\frac{\theta_c p\beta}{14.1MeV}\right)^2 \frac{x_o}{2x}}\right)$$

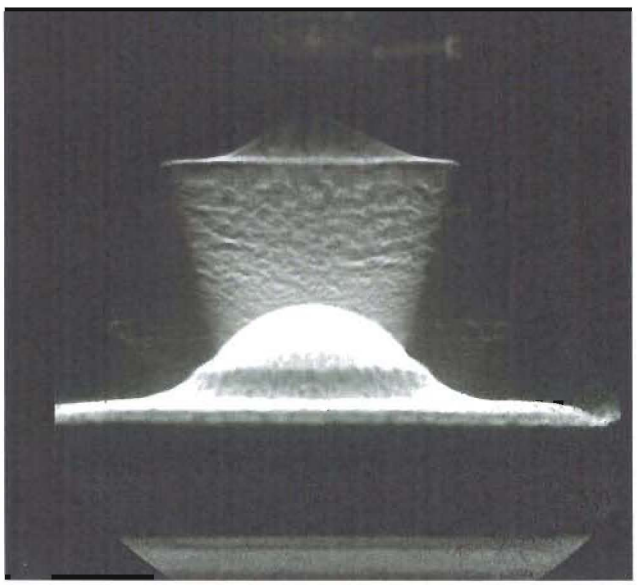

Areal Density (g/cm^2)

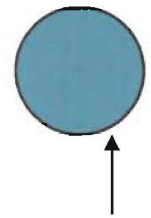

Use assumption of cylindrical symmetry to determine volume density (Abel inversion)

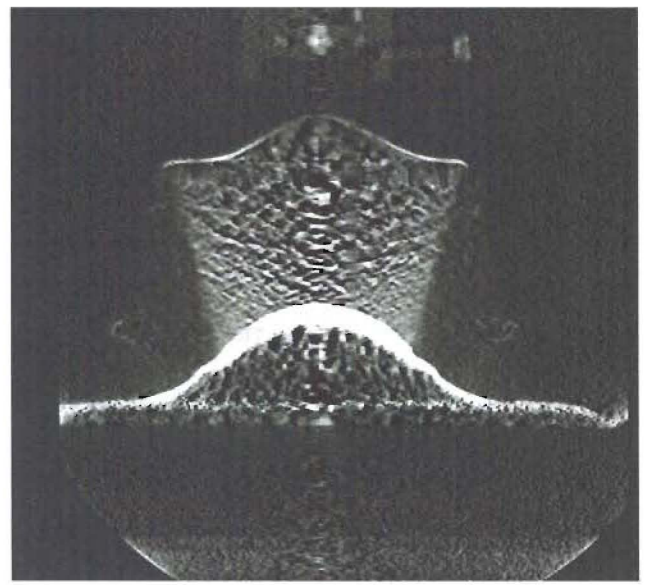

Volume Density (g/cm^3)

Proton Dark Field Imaging

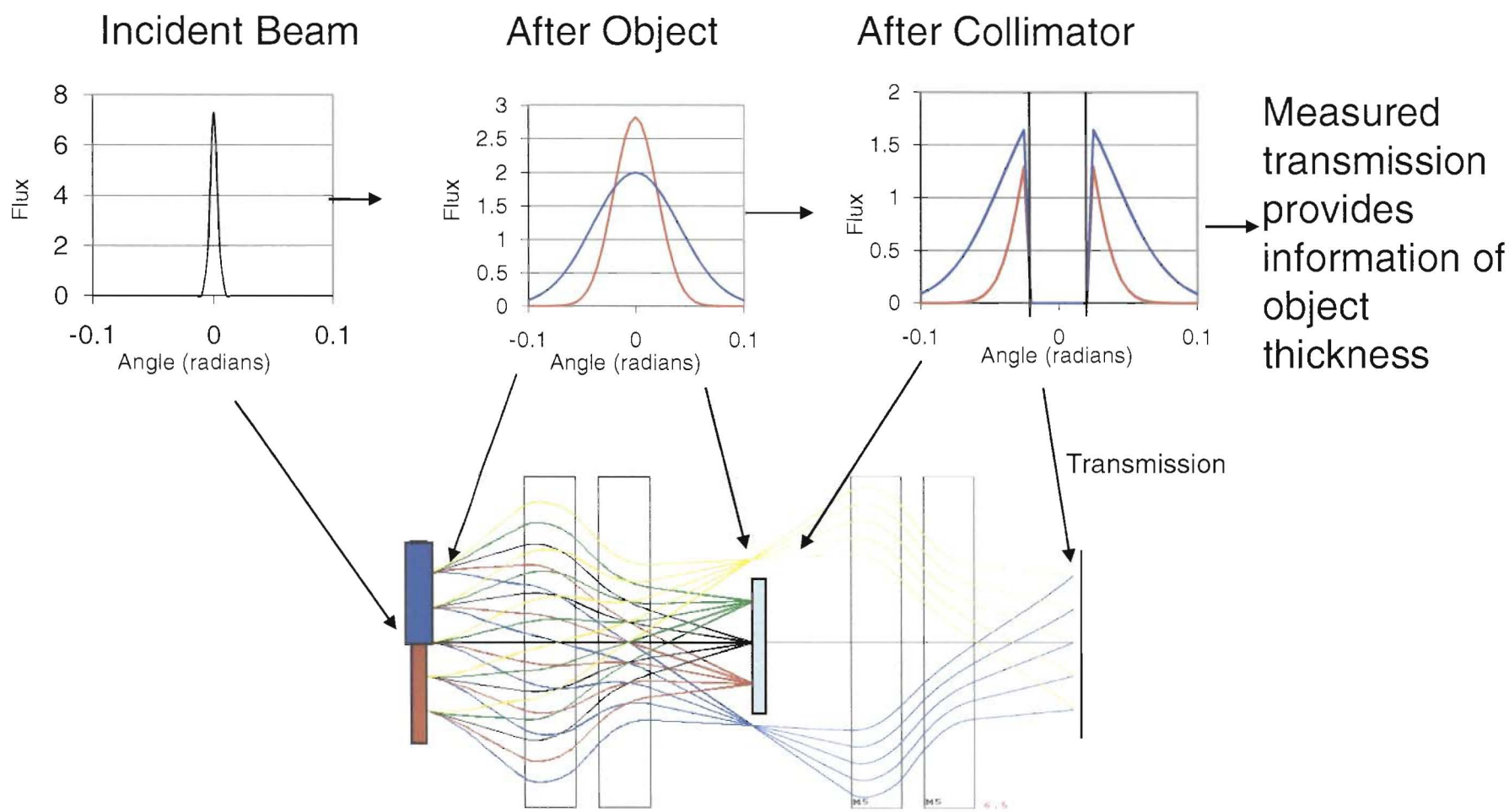

Areal Density Reconstruction

Anti-Collimator

$$T_{nuclear} = e^{-x/\lambda}$$

Nuclear removal processes

$$T_{MCS} = e^{-\theta_c^2 / 2\theta_o^2}$$

$$\theta_o = \frac{14.1MeV}{p\beta}\sqrt{\frac{x}{x_o}}$$

Multiple Coulomb Scattering with collimation:

ϑ_o - scattering angle (radians)
x - areal density
x_o - radiation length
p - momentum (MeV)
β - relativistic velocity

$$T = e^{-\left(x/\lambda + \left(\frac{\theta_c p\beta}{14.1MeV}\right)^2 \frac{x_o}{2x}\right)}$$

Total Transmission
- inverted to determine areal density, x

Radiographic Comparisons

Density Sensitivity

$$FOM = \frac{\Delta N / \sqrt{N}}{\Delta l / l} = \frac{l}{\sqrt{N}} \frac{dN}{dl}$$

Statistical sensitivity per fractional change in object thickness

800 MeV Protons*

$$N = N_0 (1 - e^{-x_c / 2l})$$

$$FOM = \sqrt{N_0} \frac{x_c}{2l} \frac{e^{-x_c / 2l}}{\sqrt{1 - e^{-x_c / 2l}}}$$

* Ignore nuclear attenuation

Dynamic Range of 800 MeV Proton Radigraphy

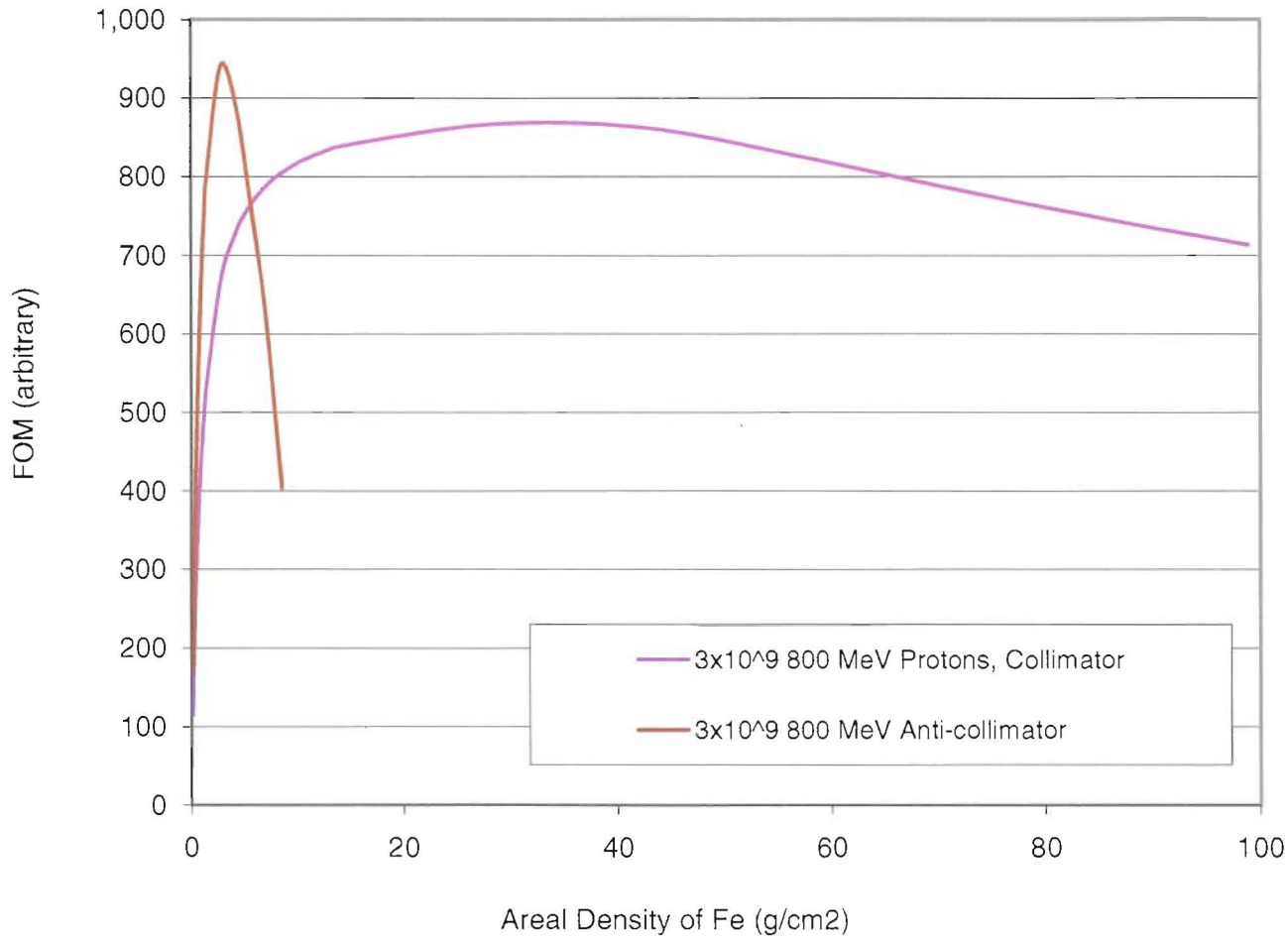

- 800 MeV proton radiography ranges from 0.05 g/cm^2 up to 50 g/cm^2

Resolution of Proton Radiography

1. **Object scattering** - introduced as the protons are scattered while traversing the object.
2. **Chromatic aberrations**- introduced as the protons pass through the magnetic lens imaging system.
3. **Detector blur**- introduced as the proton interacts with the proton-to-light converter and as the light is gated and collected with a camera system.

Assume detector development can keep up

Object Scattering

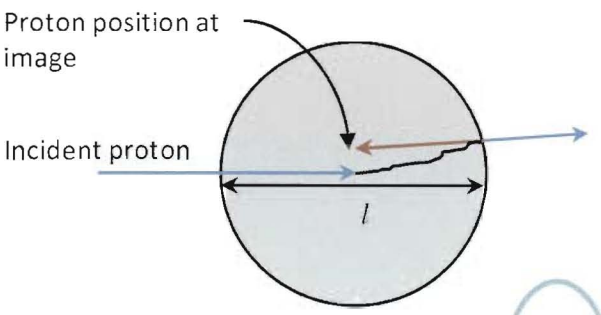

$$\sigma_o = \frac{1}{\sqrt{3}}\theta\frac{l}{2} = \frac{14.1}{\sqrt{6}}\frac{1}{P\beta}\sqrt{\frac{l^3}{x_o}} \propto \frac{l^{\frac{3}{2}}}{P}$$

Chromatic Aberrations

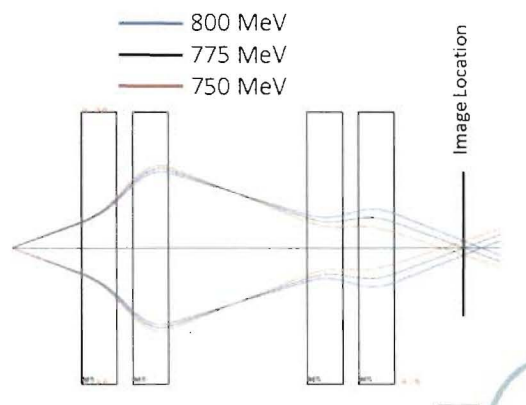

$$\sigma_c = l_c\theta\frac{\delta P}{P} = c\sqrt{P}\frac{\delta P}{P^2}\frac{14.1}{\beta}\sqrt{\frac{l}{x_o}} \propto \sqrt{\frac{l}{P^3}}$$

Detector Blur

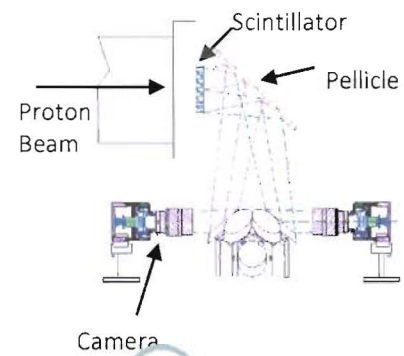

Scintillator

$$\sigma_s = \theta l_s \propto \frac{l_s\sqrt{l}}{P}$$

Camera

Resolution is independent of proton energy

Measurements of Object Scattering Blur

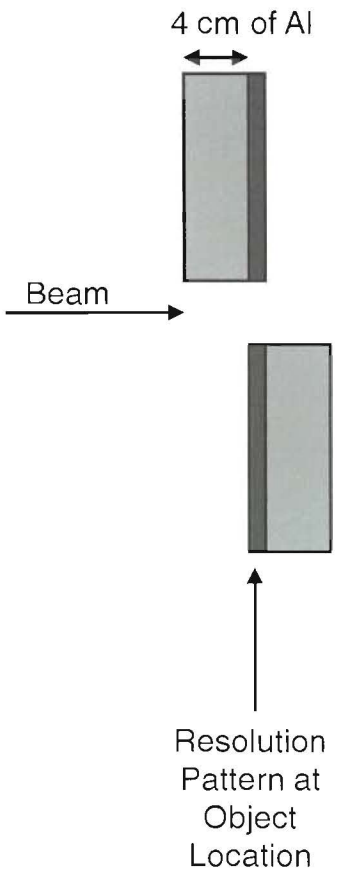

2.5 lp/mm

Sigma=0.061 mm

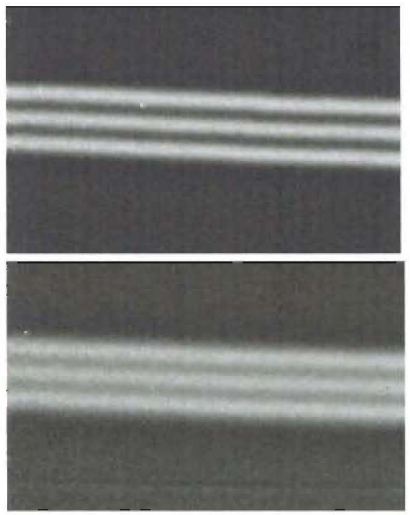

Sigma=0.150 mm

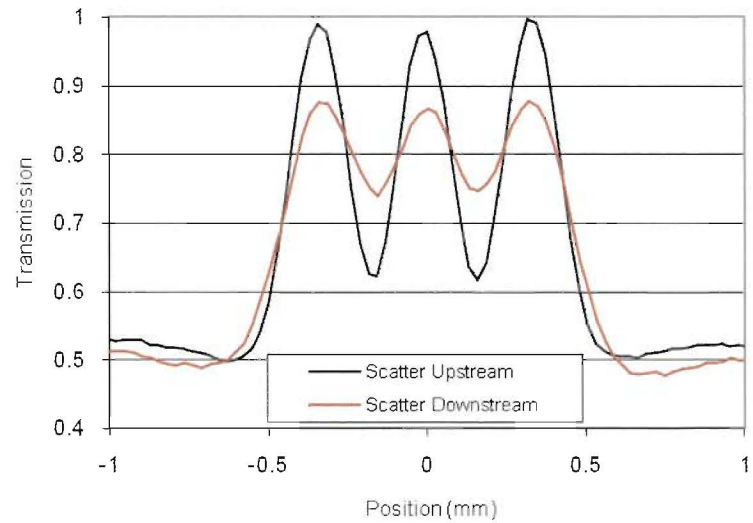

$$\sigma_o = \frac{1}{\sqrt{3}}\theta\frac{l}{2} = \frac{14.1}{\sqrt{6}}\frac{1}{P\beta}\sqrt{\frac{l^3}{x_o}} \propto \frac{l^{\frac{3}{2}}}{P}$$

Chromatic Aberration and Resolution

$$\Delta x = T_{126}\phi\delta$$

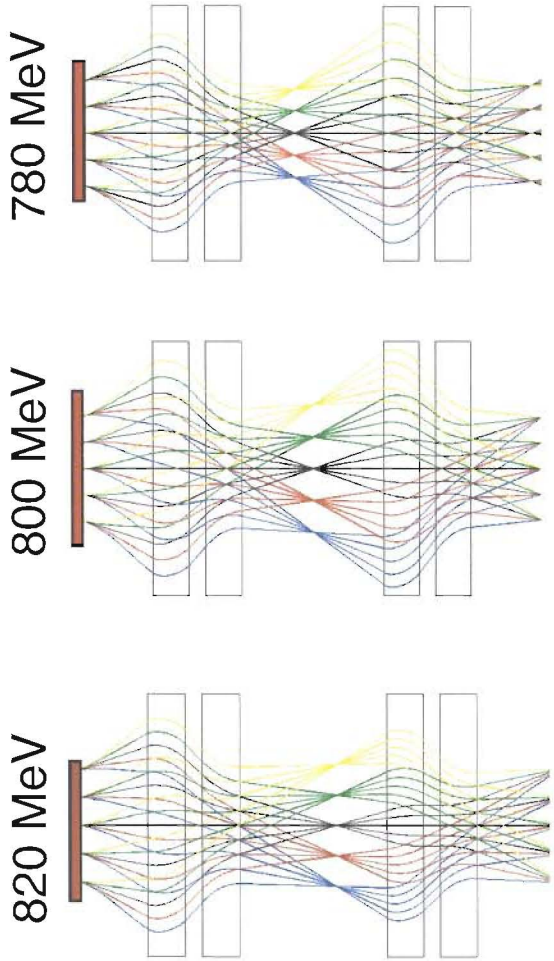

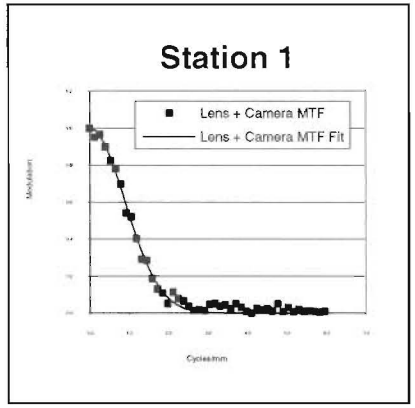

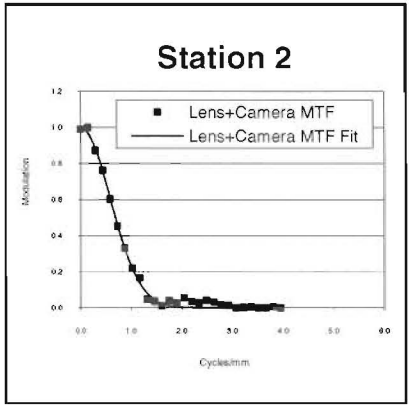

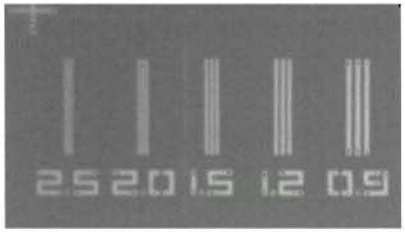

- 12 inch lens
- Station 1: 178 μm
- Station 2: 280 μm
- Gaussian blur function.
- 120 mm field of view

Thin Lens Approximation

$$\begin{pmatrix} M_{11} & M_{12} \\ M_{21} & M_{22} \end{pmatrix} = \begin{pmatrix} 1 & l \\ 0 & 1 \end{pmatrix} \begin{pmatrix} 1 & 0 \\ 1/(1+\delta)f & 1 \end{pmatrix} \begin{pmatrix} 1 & s \\ 0 & 1 \end{pmatrix} \begin{pmatrix} 1 & 0 \\ -1/(1+\delta)f & 1 \end{pmatrix} \begin{pmatrix} 1 & 2l \\ 0 & 1 \end{pmatrix} \begin{pmatrix} 1 & 0 \\ 1/(1+\delta)f & 1 \end{pmatrix} \begin{pmatrix} 1 & s \\ 0 & 1 \end{pmatrix} \begin{pmatrix} 1 & 0 \\ -1/(1+\delta)f & 1 \end{pmatrix} \begin{pmatrix} 1 & l \\ 0 & 1 \end{pmatrix} = \begin{pmatrix} -1 & 0 \\ 0 & -1 \end{pmatrix}$$

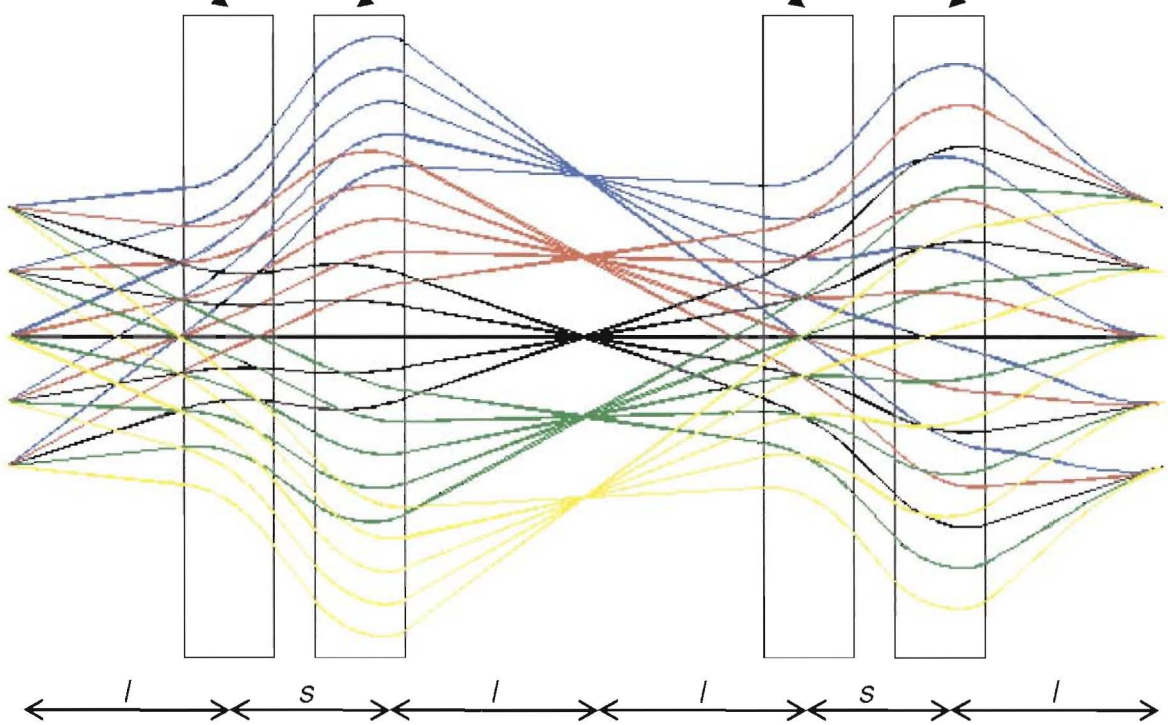

To make an identity lens

$$f = \sqrt{ls}$$

Chromatic blur is ~proportional to lens length

$$\frac{dM_{12}}{d\delta} = T_{126} = 4(l+s)$$

Chromatic Blur ⟶ Limning

Limb: To outline in clear sharp detail

Like phase-contrast radiography:

- Useful to enhance edges
- Problem for density reconstruction

Resolution proportional to energy offset

$$\sigma = C\frac{E - E_f}{E_f}\theta$$

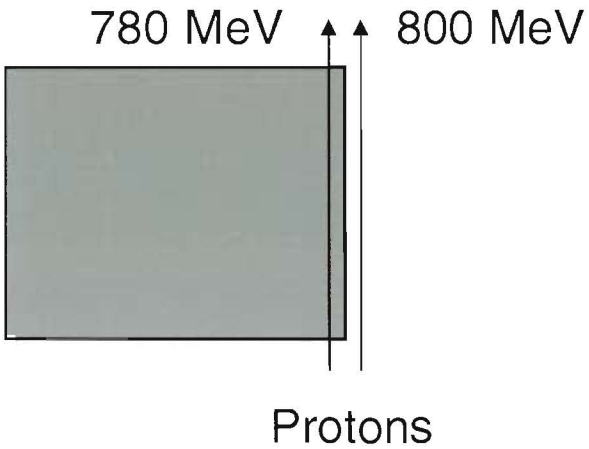

Focus on high energy protons

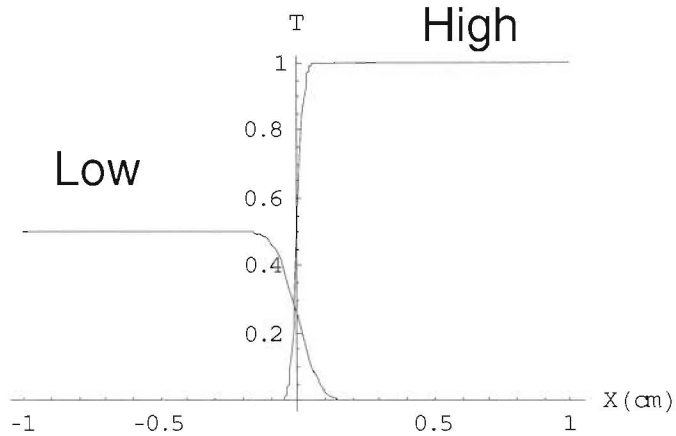

Low + High

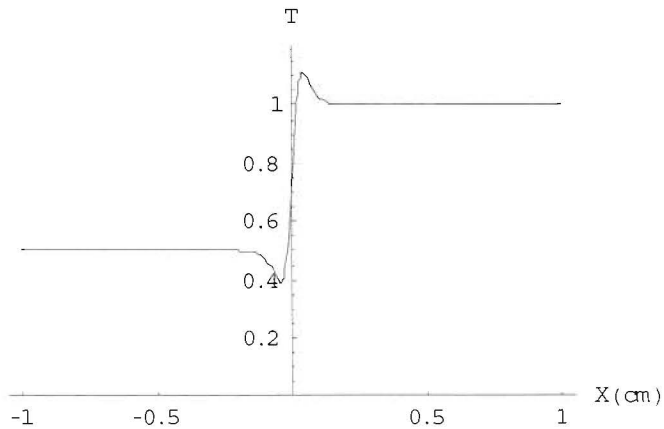

Example: Focused on high energy protons

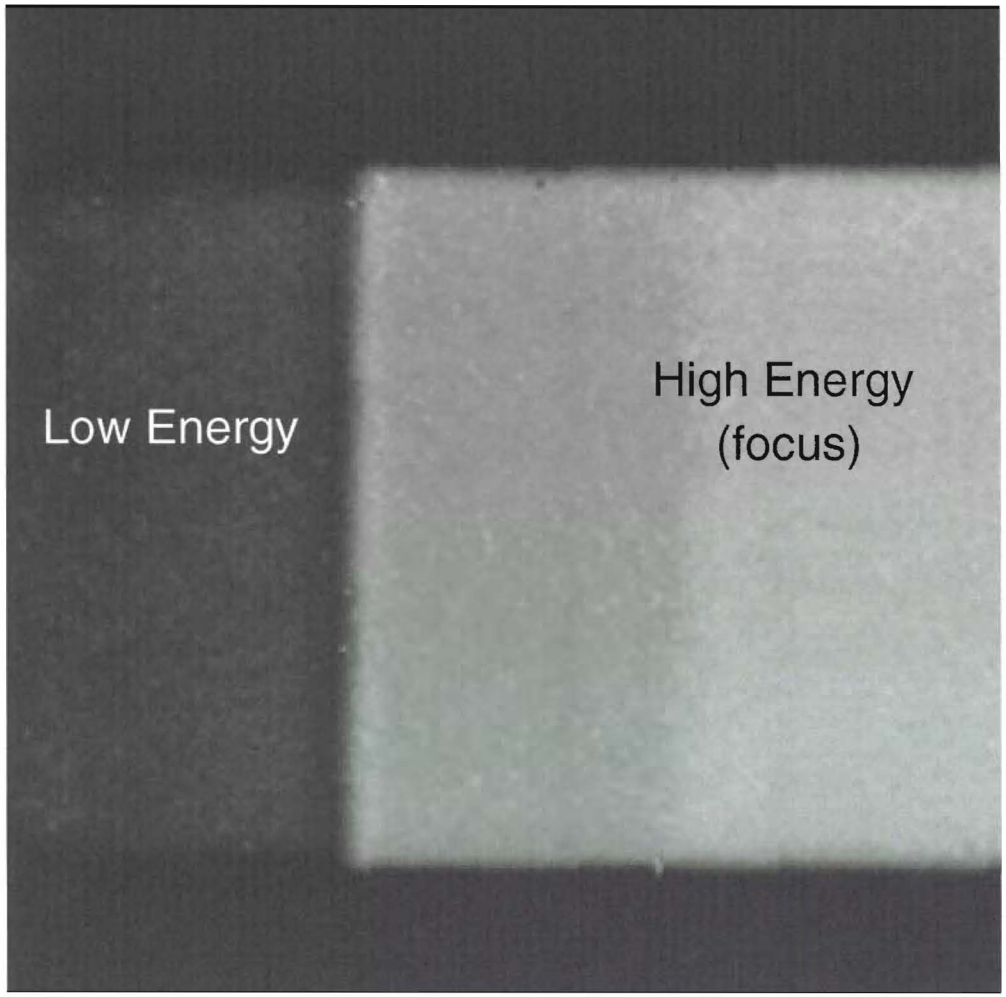

Focus on high energy protons

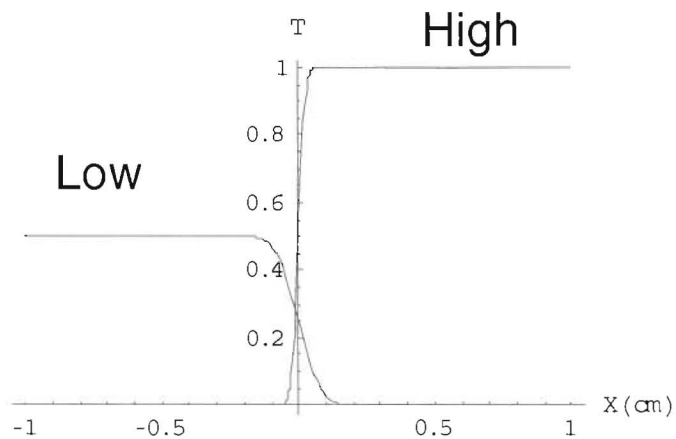

Low + High

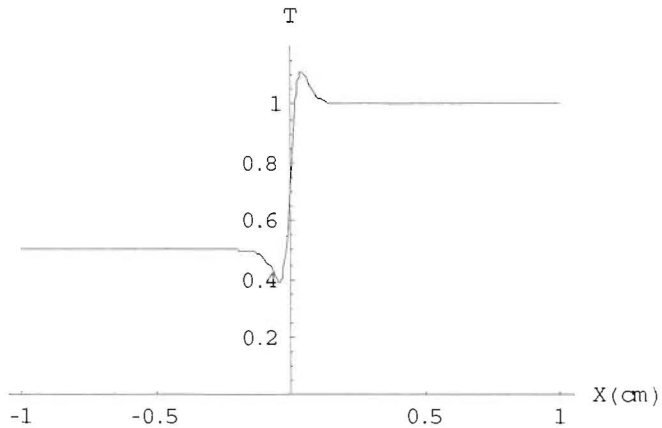

Results of Scaling 800 MeV Resolution

Resolution: RMS of a ~Gaussian distribution
No Detector Blur

High Explosives

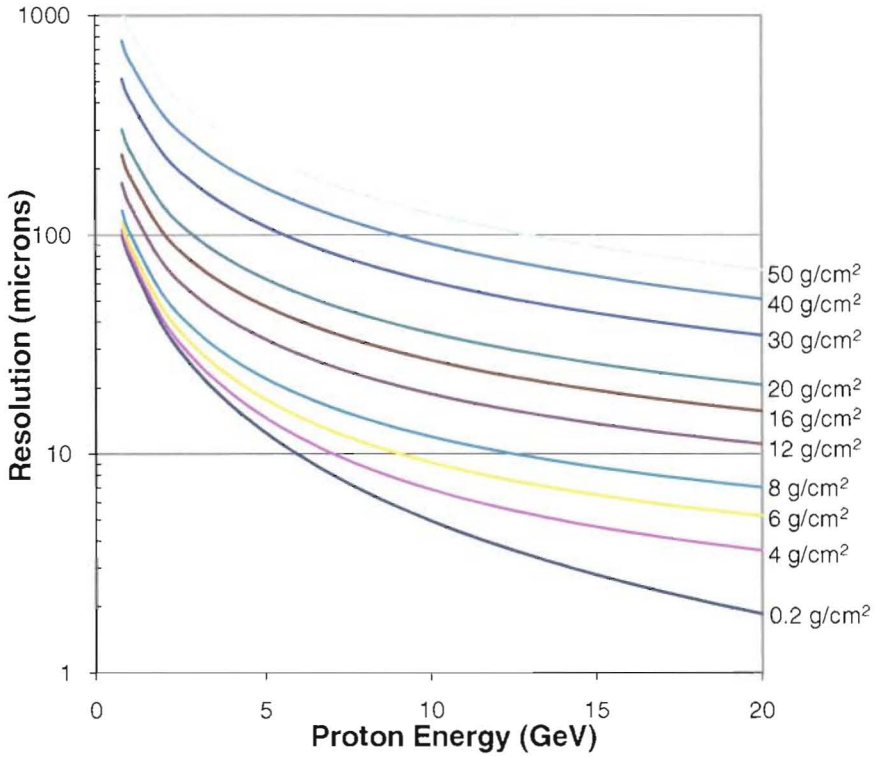

Uranium

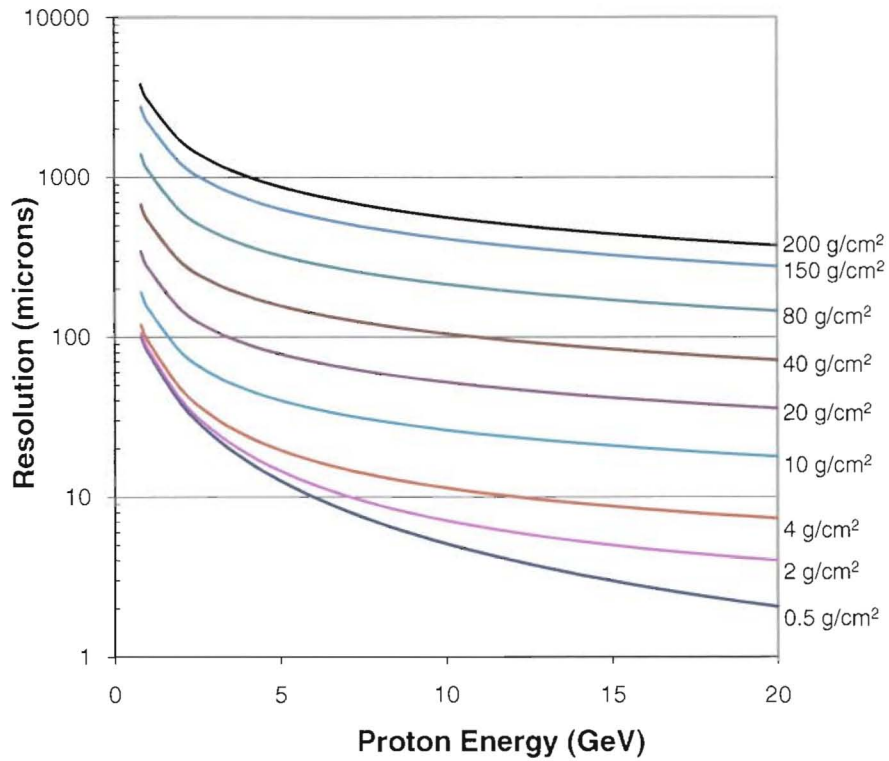

<u>4 GeV Protons</u>
25-350 micron resolution in HE
25-1000 micron resolution in Uranium

<u>20 GeV Protons</u>
2-100 micron resolution in HE
2-350 micron resolution in Uranium

Comparison of Scaling to a Measurement

Scaling is a factor of 2-3 too conservative.

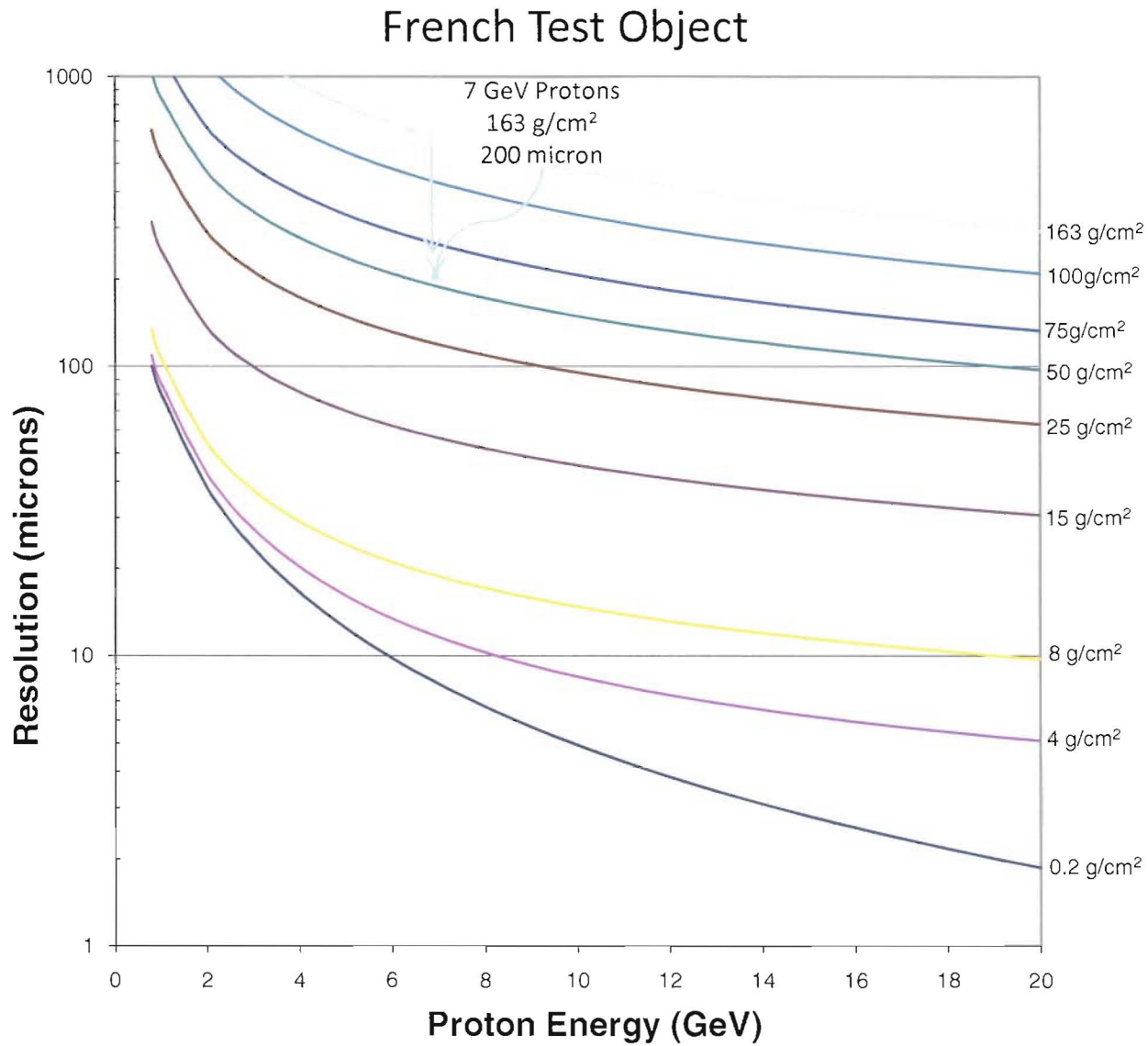

800 MeV Magnifying Imaging Lens

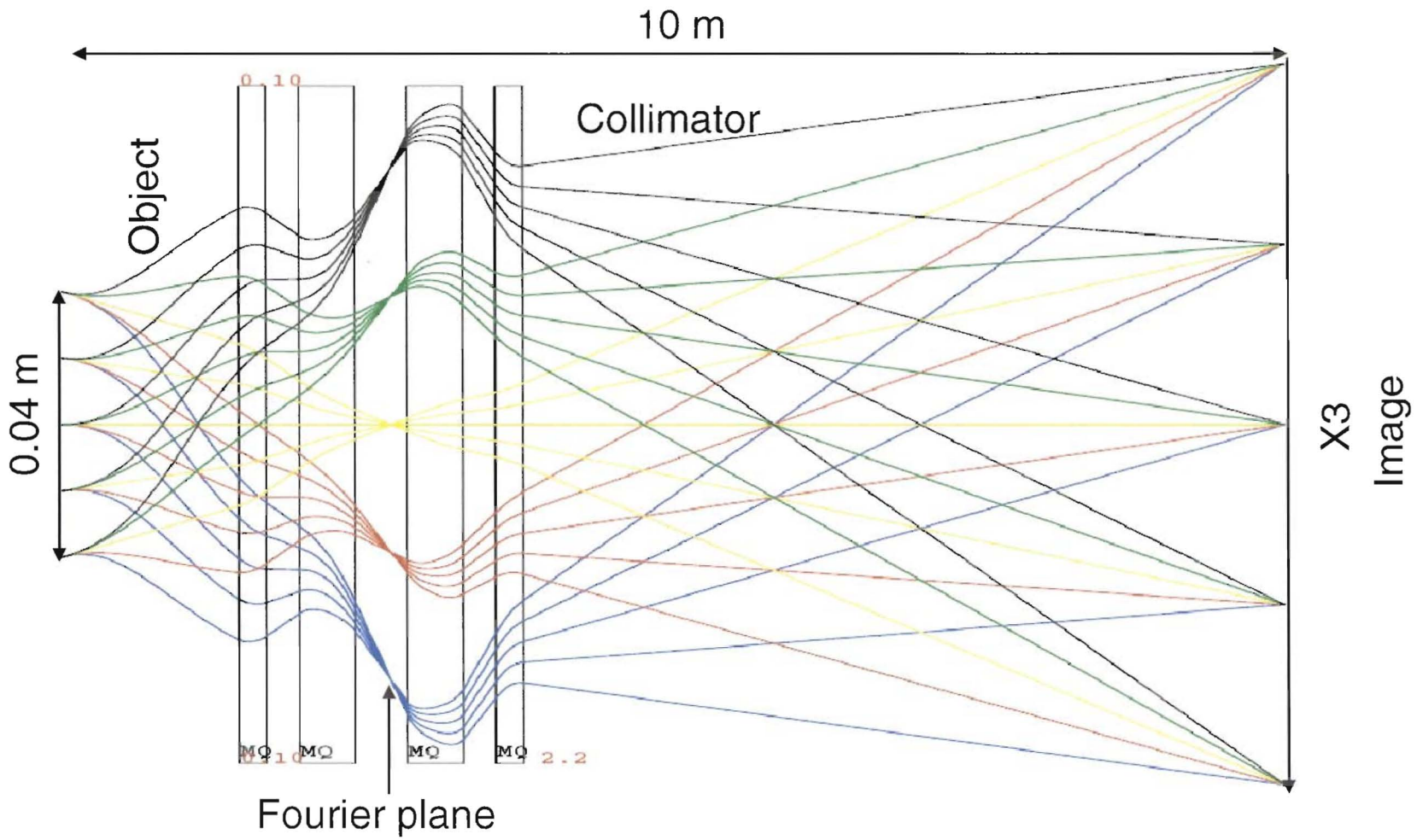

Thin Lens Approximation

$$\begin{pmatrix} M_{11} & M_{12} \\ M_{21} & M_{22} \end{pmatrix} = \begin{pmatrix} 1 & z \\ 0 & 1 \end{pmatrix} \begin{pmatrix} 1 & 0 \\ 1/(1+\delta)f & 1 \end{pmatrix} \begin{pmatrix} 1 & s \\ 0 & 1 \end{pmatrix} \begin{pmatrix} 1 & 0 \\ -2/(1+\delta)f & 1 \end{pmatrix} \begin{pmatrix} 1 & b \\ 0 & 1 \end{pmatrix} \begin{pmatrix} 1 & 0 \\ 2/(1+\delta)f & 1 \end{pmatrix} \begin{pmatrix} 1 & s \\ 0 & 1 \end{pmatrix} \begin{pmatrix} 1 & 0 \\ -1/(1+\delta)f & 1 \end{pmatrix} \begin{pmatrix} 1 & l \\ 0 & 1 \end{pmatrix} = \begin{pmatrix} -1 & 0 \\ 0 & -1 \end{pmatrix}$$

$$f = 2\sqrt{\frac{lms + (m-1)s^2}{(m+1)}}$$

$$z = lm + 2(m-1)s$$

$$b = \frac{2s\left(lm + (m-1)\right)}{m(l+2s)}$$

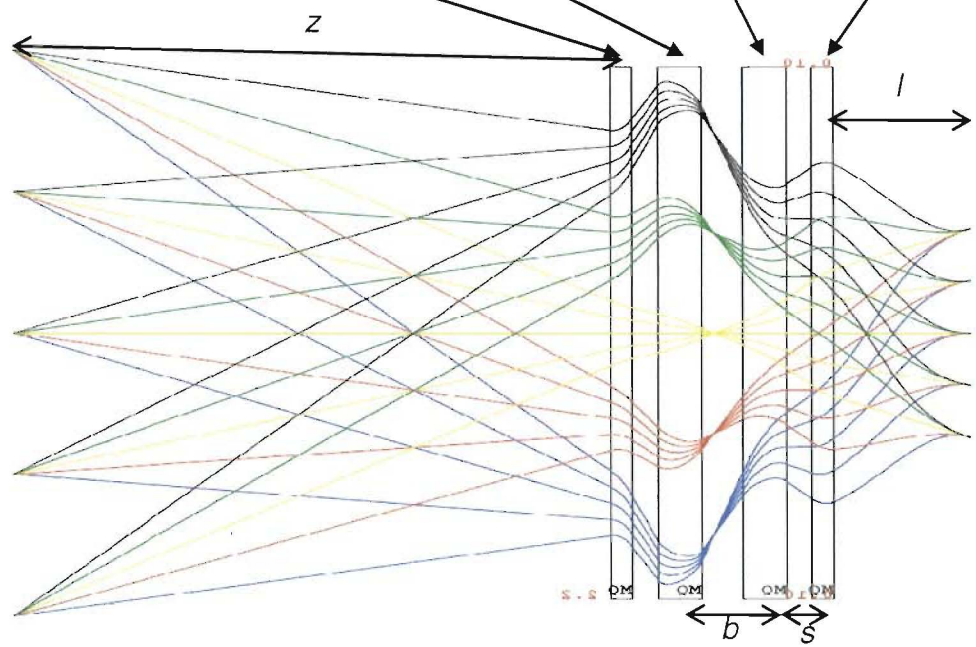

$$\frac{1}{m}\frac{dM_{12}}{d\delta} = \frac{T_{126}}{m} = \frac{m+1}{m^2\left(lm + (m-1)s\right)}\left[(2l^2m^2 + lm(5m-3)s + 2(m-1)s^2\left((2m-1) + \sqrt{(m+1)(lm+(m-1)}\right)\right]$$

Chromatic blur is a complicated function of lens spacing

$$\frac{T_{126}}{m} \cong 2l + \frac{l}{m}$$ In the limit that $\frac{s}{l} \ll 1$

X3 Magnifier Resolution

- 65 μm RMS resolution
- Approximately Gaussian Point spread function

2.5 lp/mm

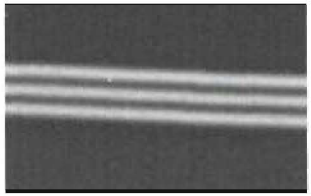

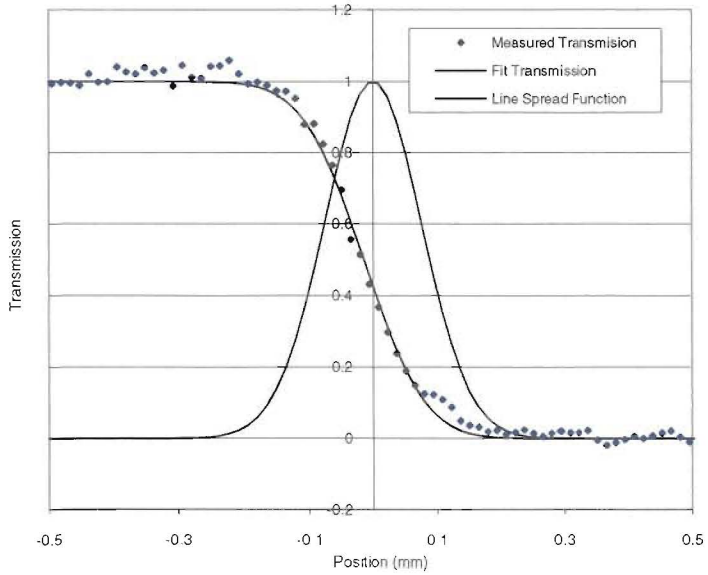

Resolution Versus Magnification

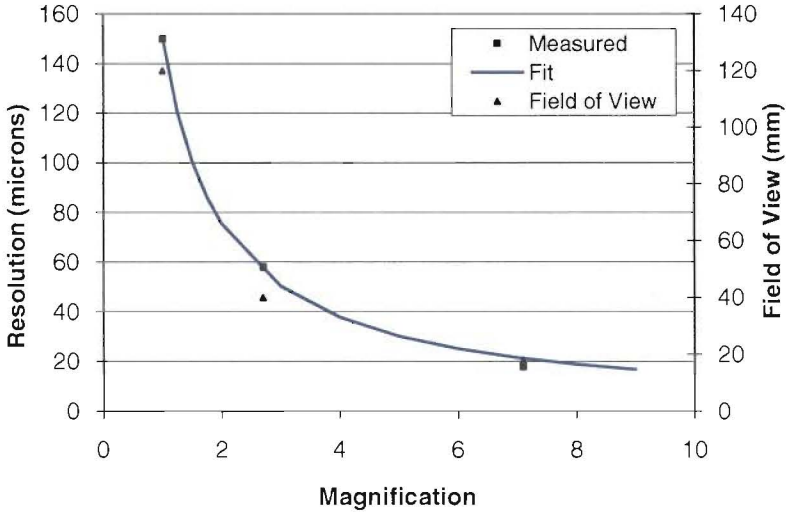

Commissioning of the pRad Microscope System

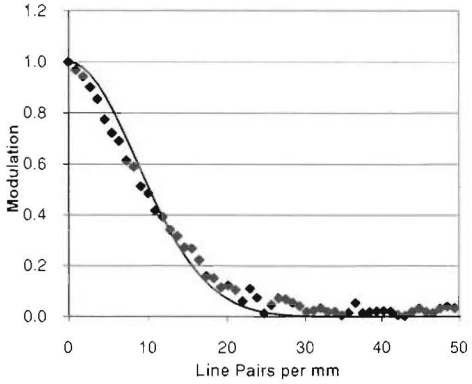

- X7.1 Magnification
- 18 mm field of view
- 18 μm resolution
- Radiographs at 9 times

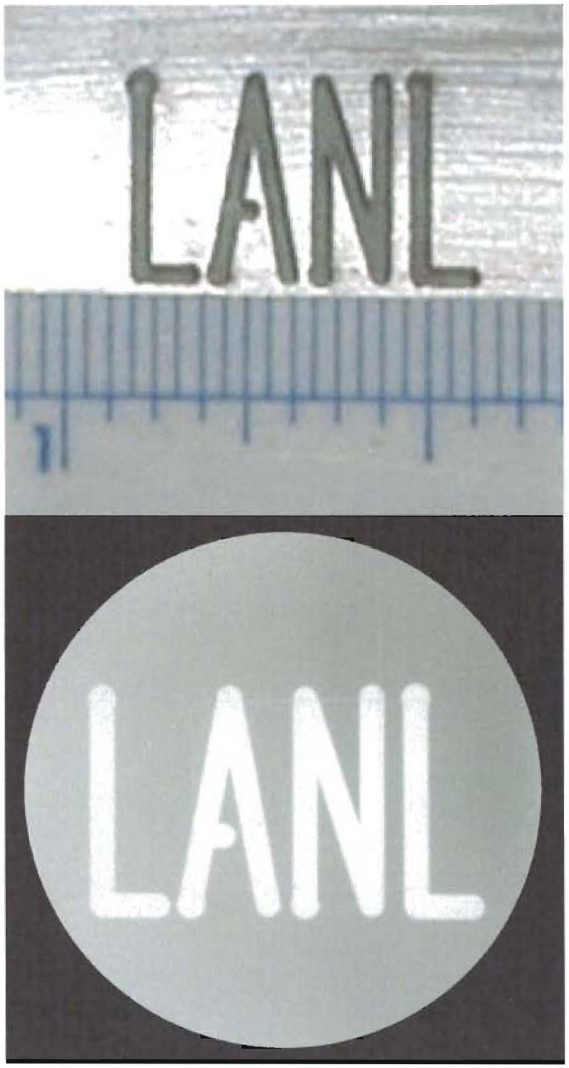

Solid-Solid Phase Transition in Iron

(X3 Magnifier)

Dramatic Improvement in Resolution is allowing us to make new measurements like this solid-solid phase transition in iron. We are performing experiments with the magnifier to study solid-solid phase transitions in cerium this week.

Identity Lens $\frac{\Delta P}{P} = 8.7\%$

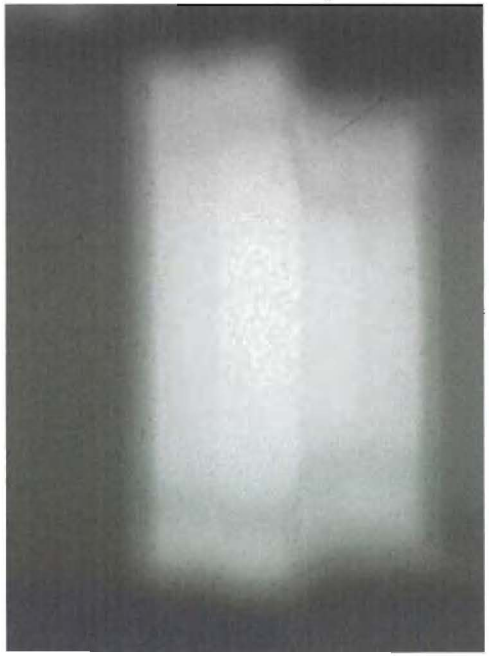

copper

X3 Magnifying Lens $\frac{\Delta P}{P} = 8.1\%$

Iron

Resolution improvement equivalent to an energy increase from 800 MeV to 2 GeV (in terms of chromatic blur)

Combine Higher Energy with Magnification

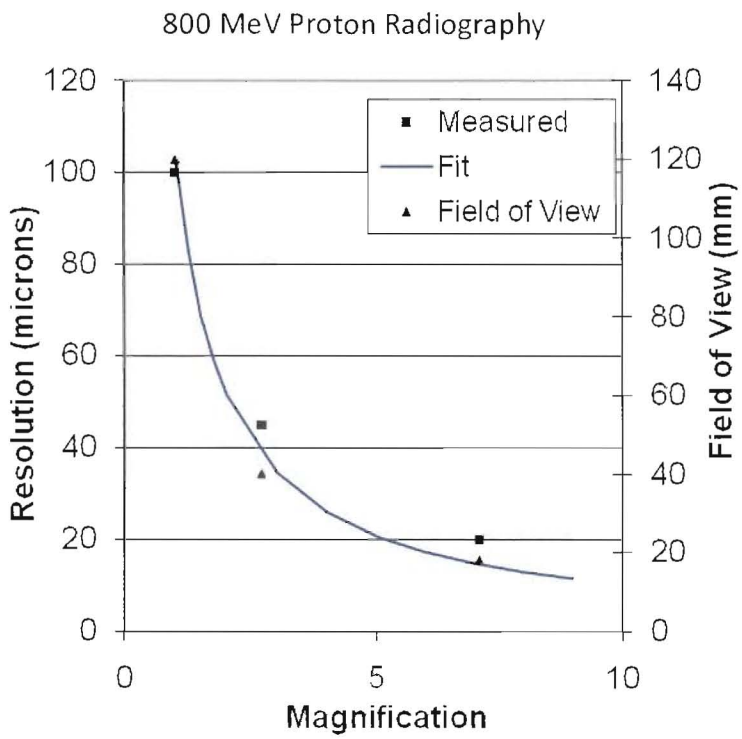

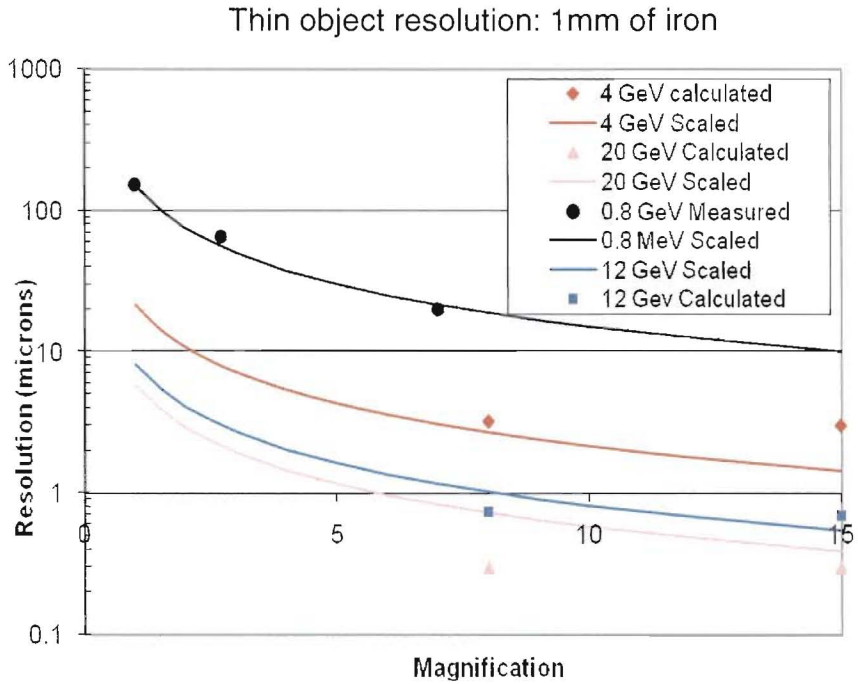

Magnification at high energy could result in high resolution (<1 micron?) with a 20 mm field of view

Simple Figure of Merit Comparison

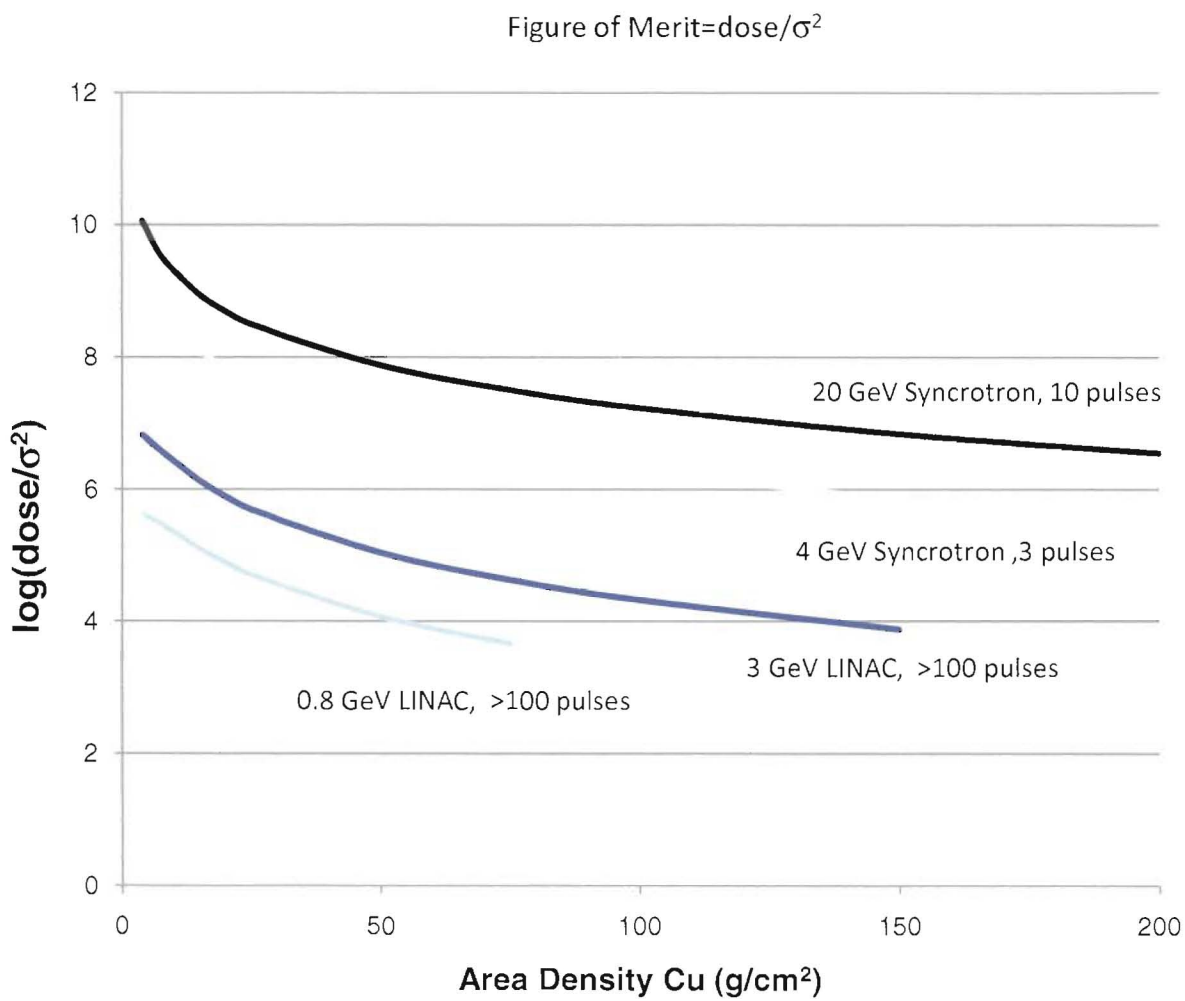

Material Strength Experiments (Olson Series)

(X3 magnifier)

PTW fit to Hopkinson-Bar data*

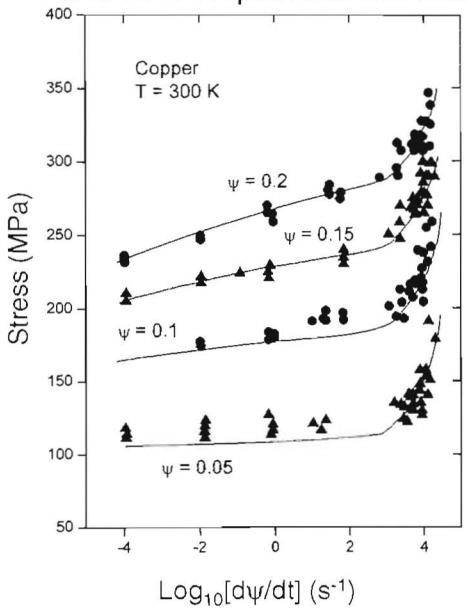

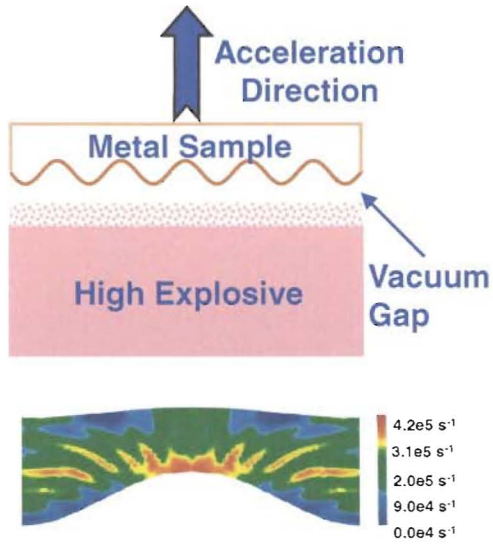

Calculated Strain Rate

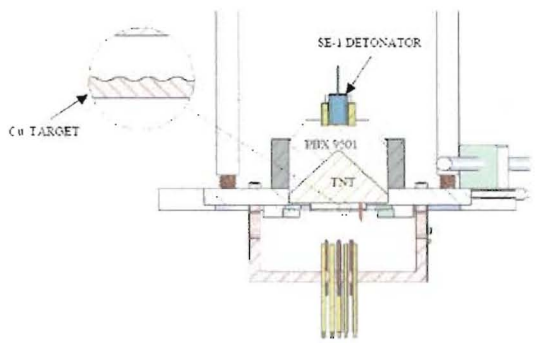

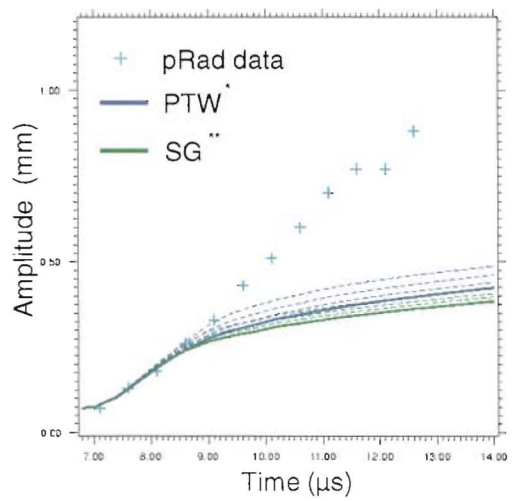

2 mm offset 3 mm offset

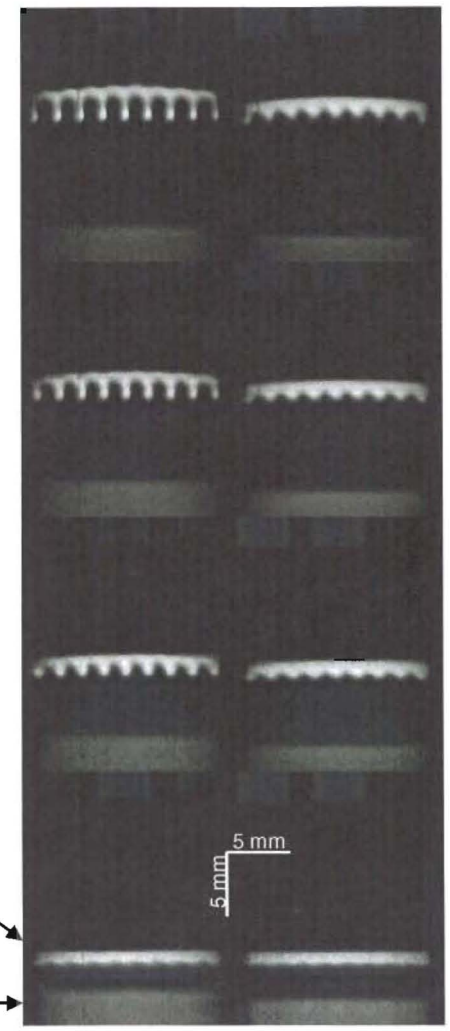

*D.L.Preston, et al. J.Appl. Phys. **93**, 211 (2003). ** D. J. Steinberg, et al. J.Appl. Phys. **61**, 1816 (1987).

Powder Gun Al/Cu Equation Of State

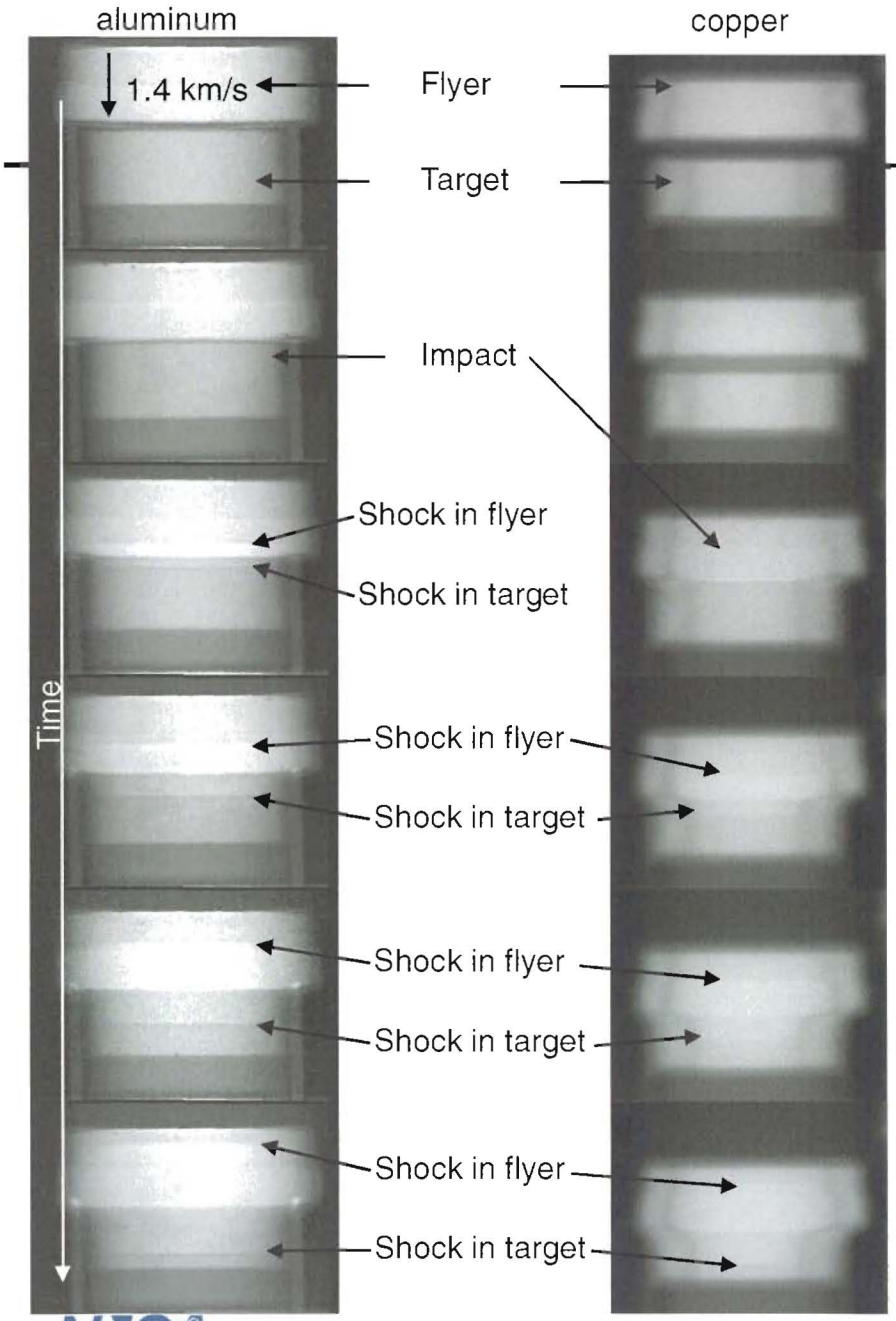

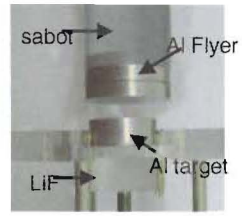

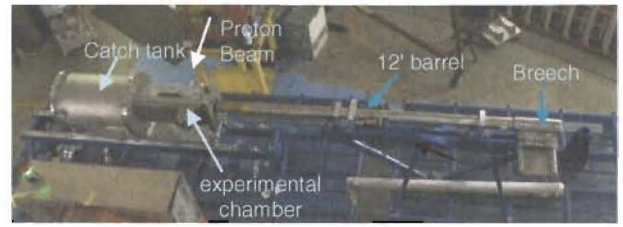

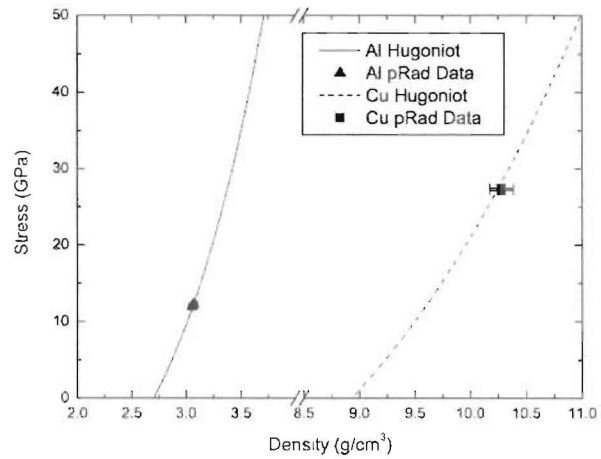

TABLE I. Summary of the experiments with the uncertainties for each quantity shown in parentheses.

Experiment	Impactor/ sample	Impactor velocity (mm/μs)	Peak stress (GPa)	Initial density (g/cm³)	Calculated density (g/cm³)	Measured density (g/cm³)	Agreement
1	Al 6061-T6	1.452 (0.012)	12.27 (0.11)	2.710 (0.003)	3.067 (0.005)	3.070 (0.025)	0.1%
2	Al 6061-T6	1.422 (0.002)	11.98 (0.03)	2.710 (0.003)	3.060 (0.004)	3.056 (0.020)	0.1%
3	OFHC Cu	1.30 (0.04)	28.59 (0.91)	8.928 (0.003)	10.30 (0.05)	10.28 (0.08)	0.2%
4	OFHC Cu	1.249 (0.002)	27.16 (0.06)	8.928 (0.003)	10.241 (0.006)	10.28 (0.08)	0.4%

Solid-Solid Phase Transitions in Iron

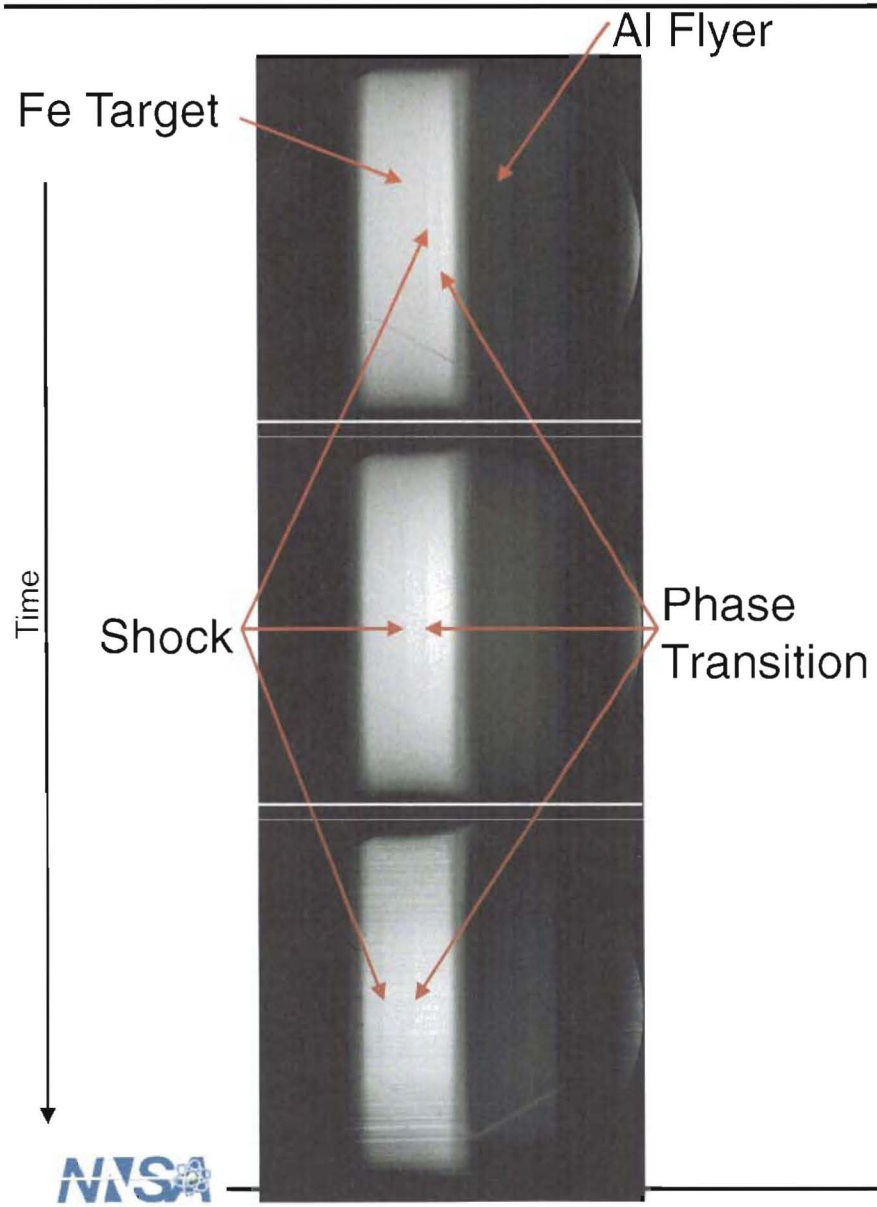

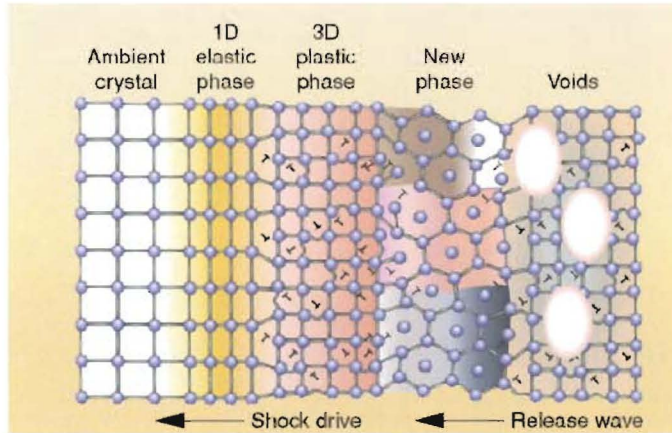

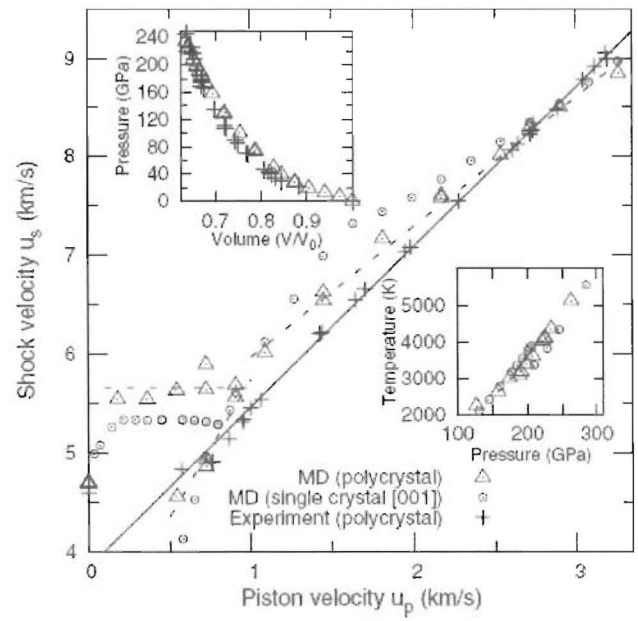

Phys. Rev. Lett. 98 135701 (2007)

pRad has been used to study the failure of materials driven by point detonated high explosives

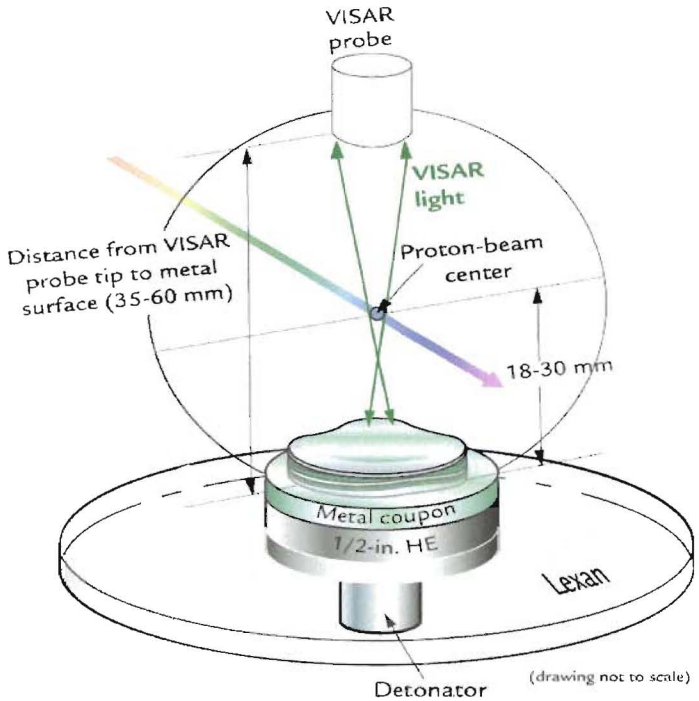

A comparison of spall for different materials

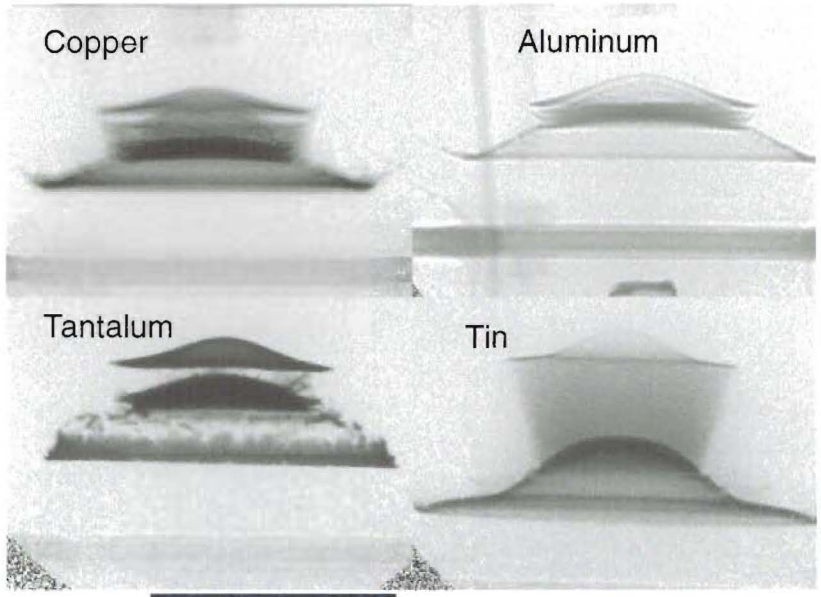

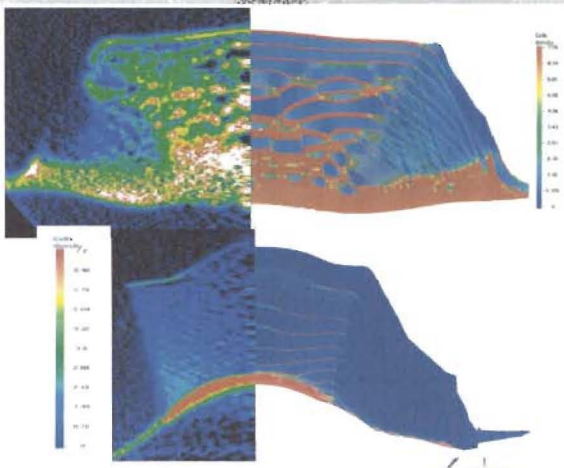

- Experiments were aimed at extending VISAR measurements below the leading spall layer.
- Proton radiographs reveal that the deepest damage layers are not well defined.
- Multiple pRad experiments show that damage formation deep within the metal is "statistical" in nature and dependent on metal.

The origins of eRad

"Okay. Now that we know bombarding the sample with *croutons* isn't the answer, what say we try **Electrons.**

30 MeV Electron Microscopy

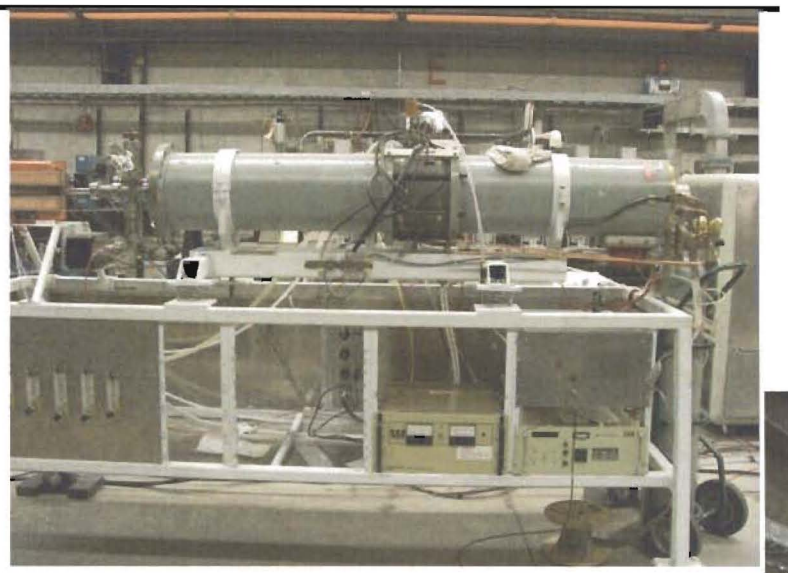

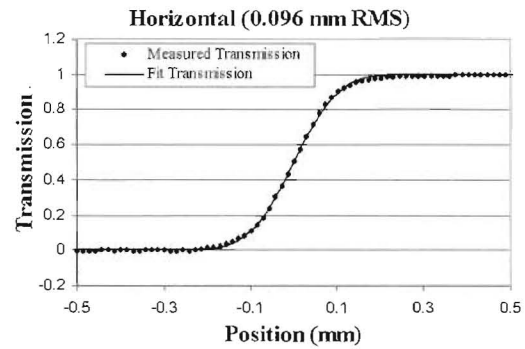

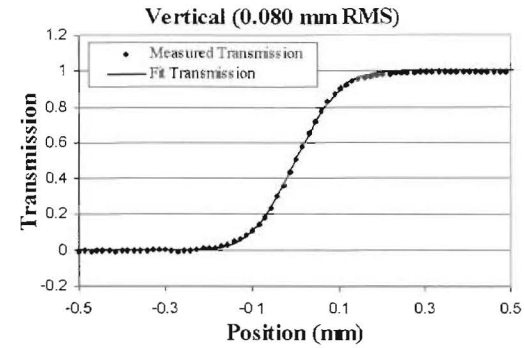

Radiograph of the tungsten filament from a small light bulb. The filament is made from a 0.025 mm tungsten wire.

Radiograph of a fishing fly. The feather material has areal densities of >0.5 mg/cm^2 and is 0.1-1 mm in diameter.

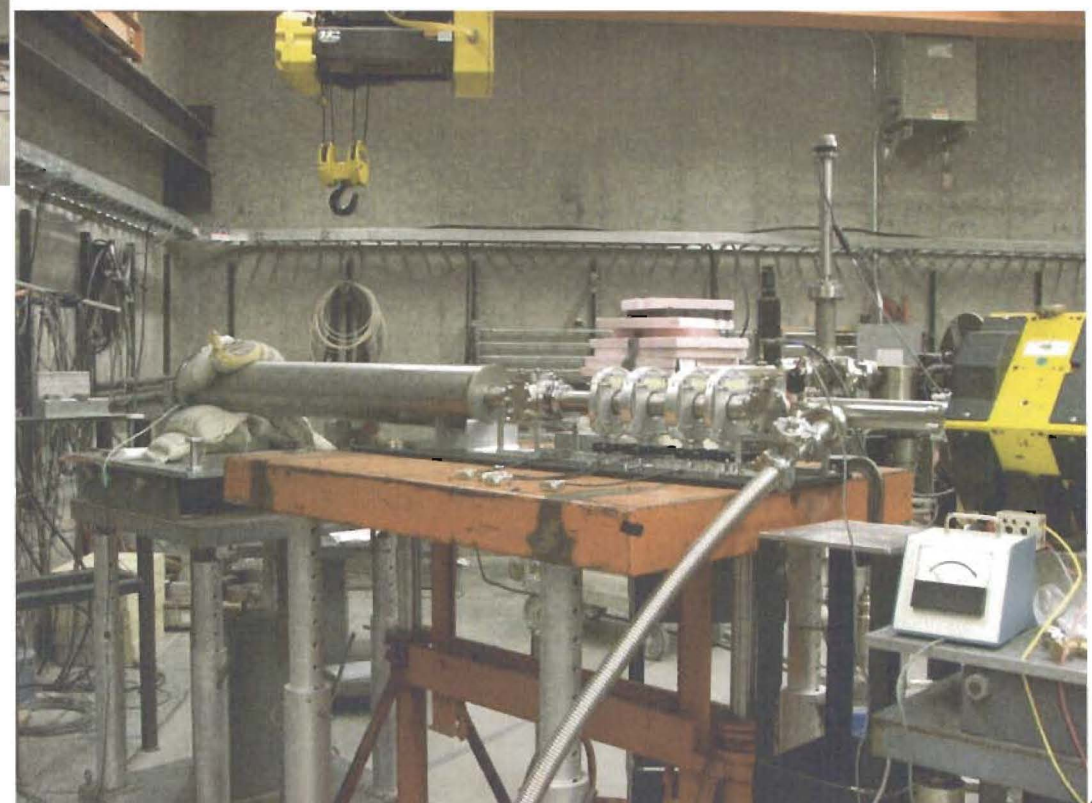

Density Resolution

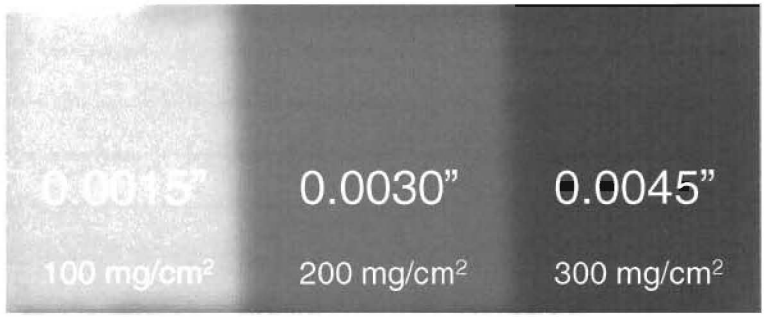

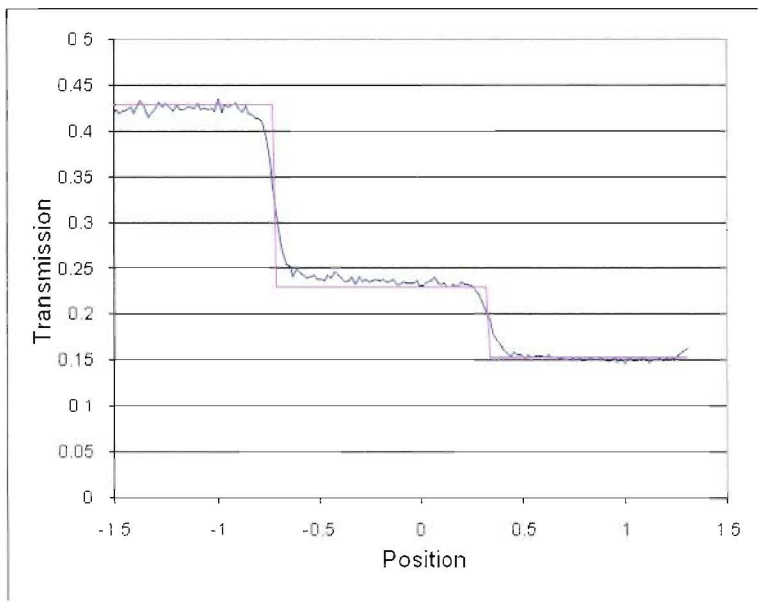

- Measured transmission through one aluminum step wedge.
- Measurement is in reasonable agreement with calculations
- Need to develop a method to accurately measure beam energy.
- Need to collect data with step wedges of various thicknesses and materials.
- Need to determine how low in transmission results in a useful density measurement.

Sensitivity

Hand written "eRad"

- 1" wide
- Pilot "Golden Pen" ink containing 17% copper (<0.001 thick)
- 5×10^{11} electrons

Magnetic field of a refrigerator magnet

- ~500 Gauss field at magnet surface
- Electrons deflected by the B field are intercepted at the collimator location.

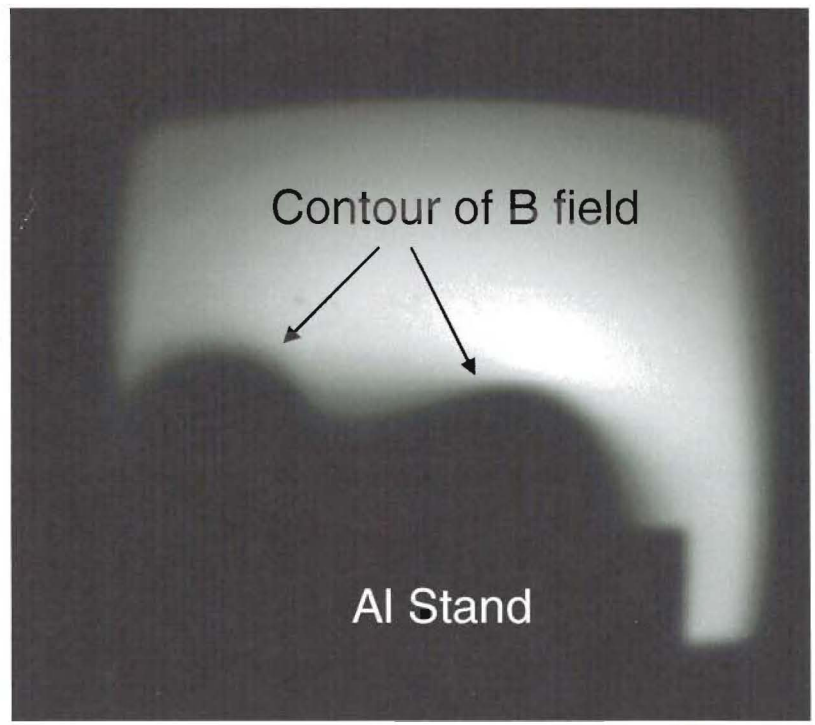

Proton-Electron Comparison

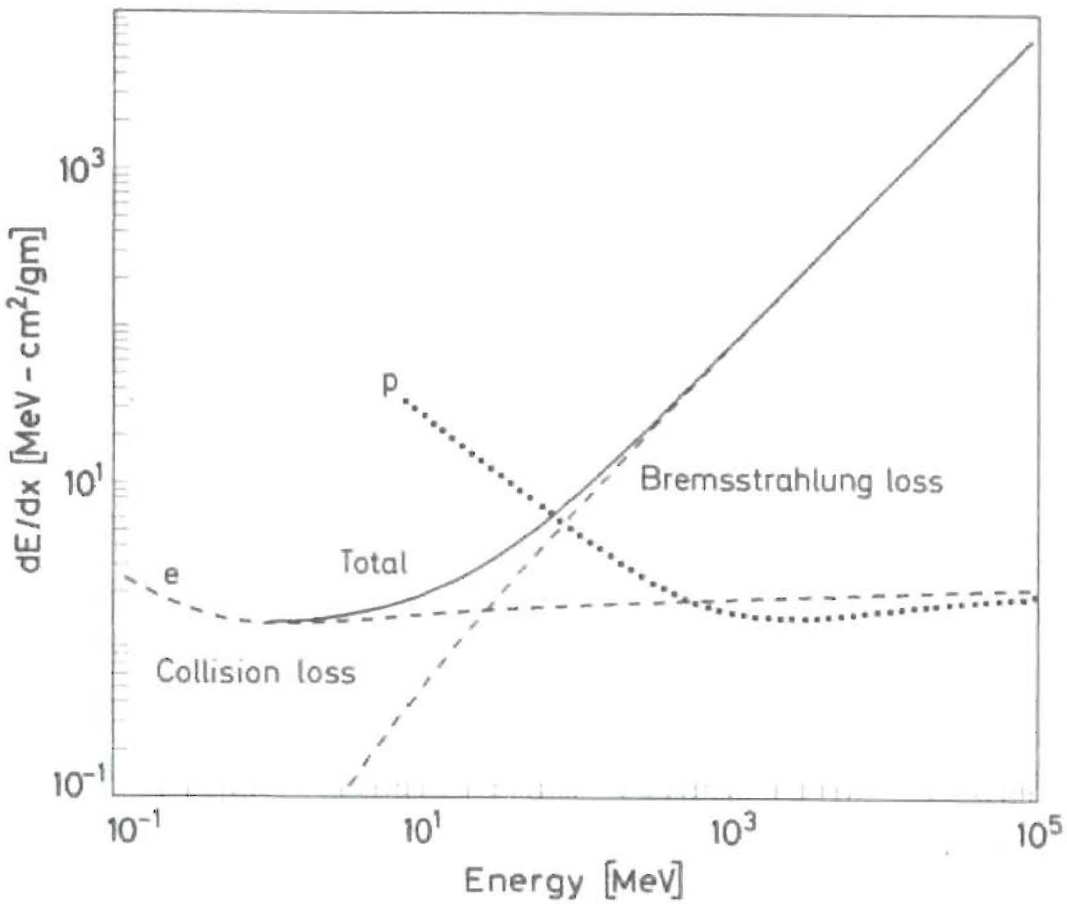

dE/dx linearly increases for electrons above critical energy. Typically ~30 MeV. Therefore, dP/P for Bremsstrahlung interacting electrons does not decrease with higher energy.

dE/dx nearly constant (logarithmically increasing) for protons above 1 GeV. Therefore, dP/P decreases with higher energy improving chromatic aberrations.

Question: Are there enough non-Bremsstrahlung interacting, forward electrons to make useful radiographs?

Energy spectrum of electrons reaching the image location

1 mm Fe cube radiographed with 35 GeV electrons

Long-range blur

Point Spread Function

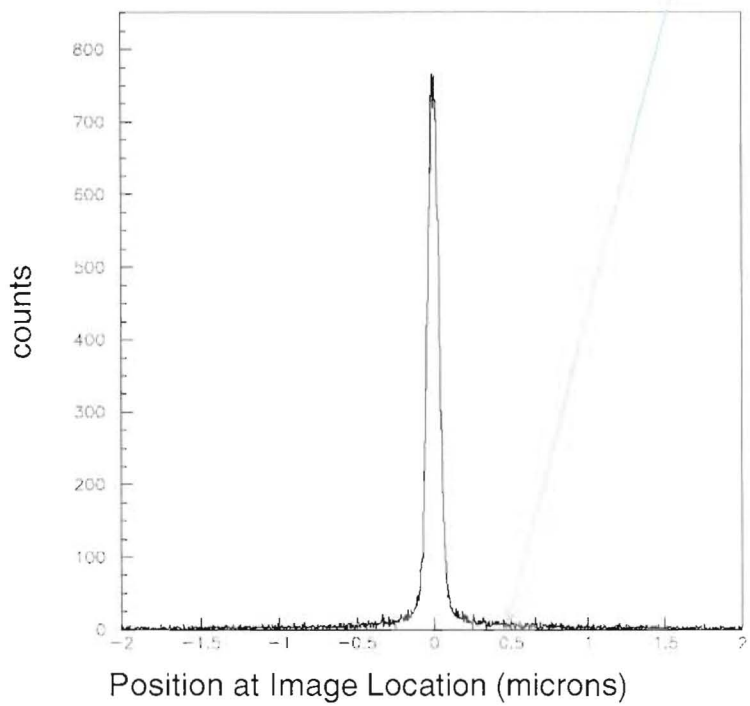

100 nm FWHM

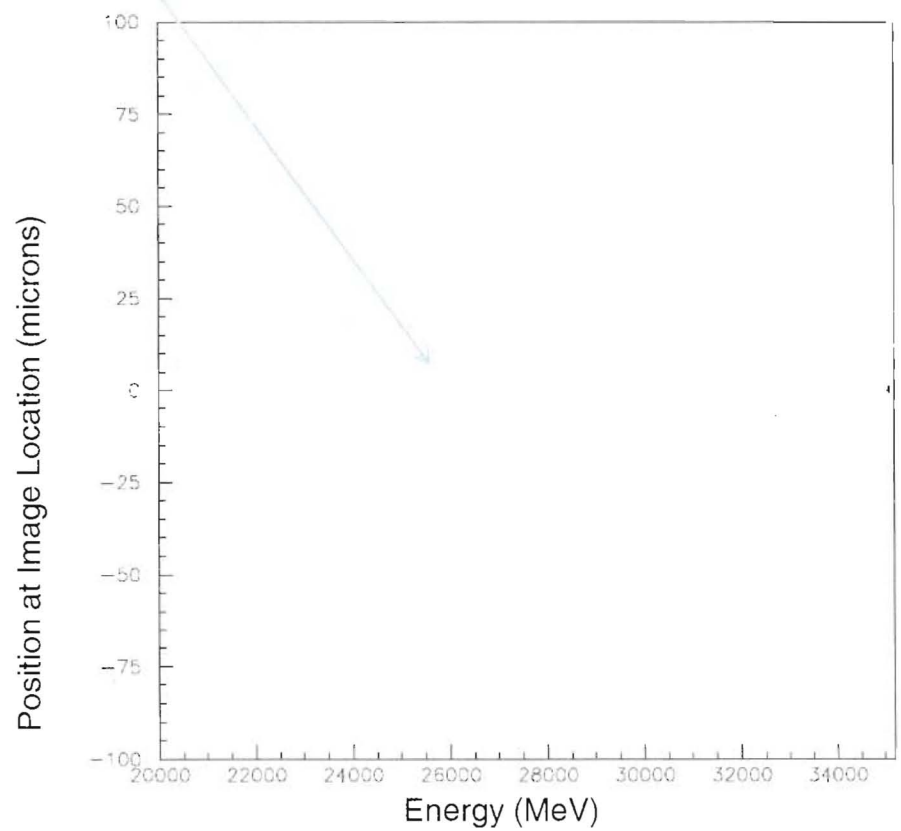

What energy electrons do you need?

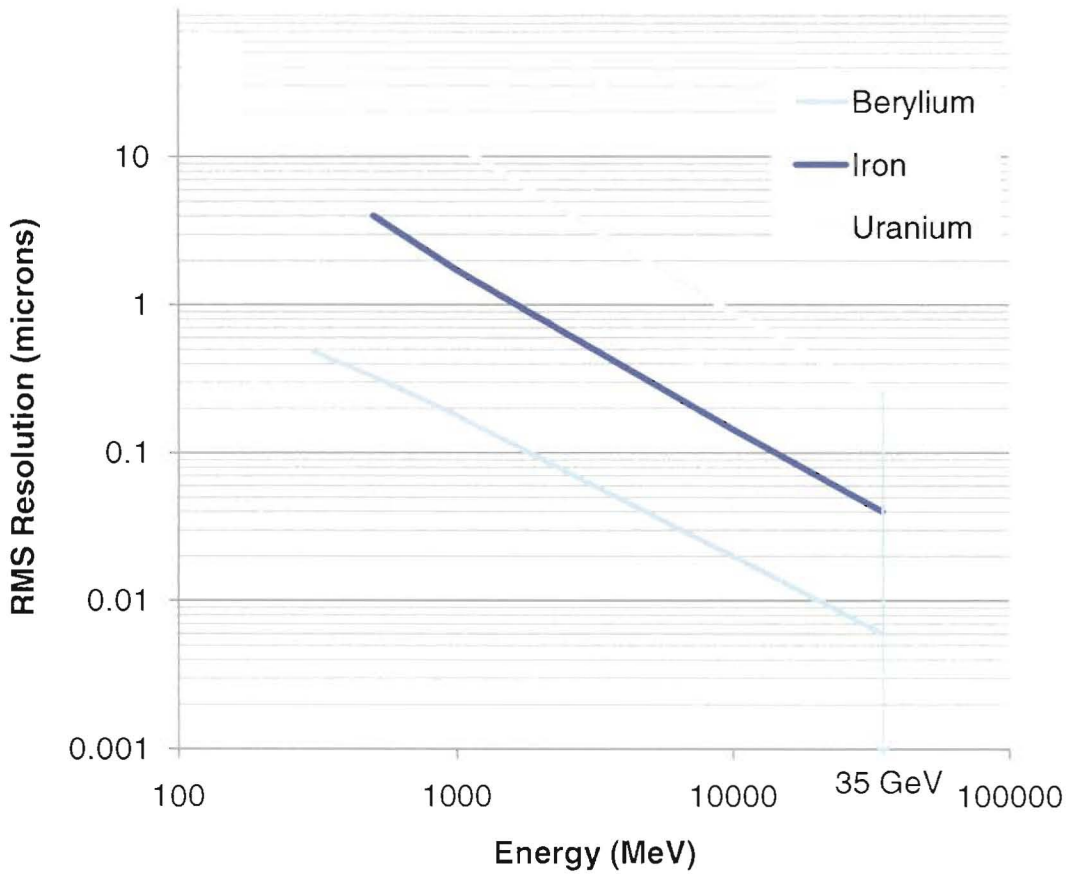

Iron point spread function

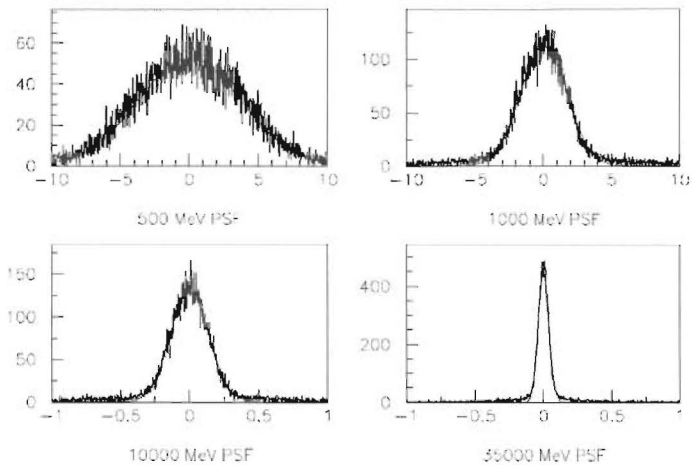

Uranium point spread function

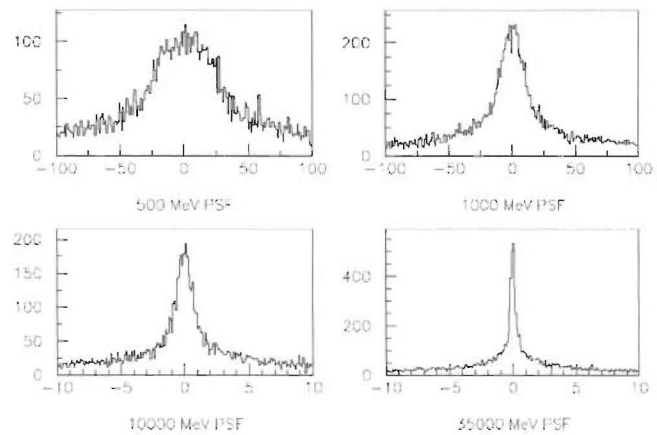

How thick an object?

Iron Object of Various Thicknesses

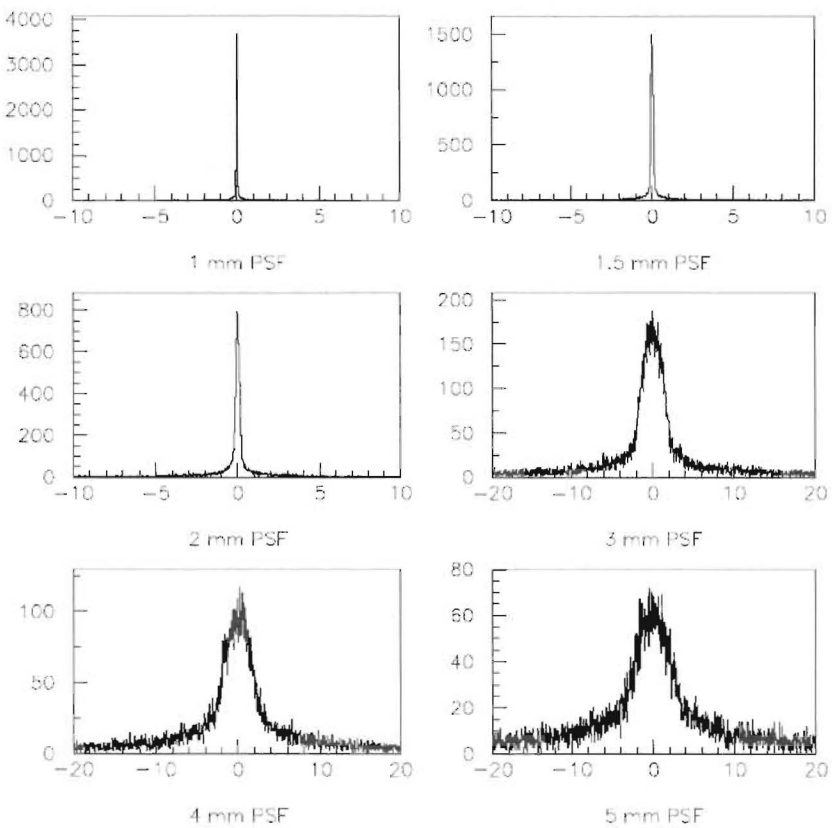

~RMS width of "core" through Iron

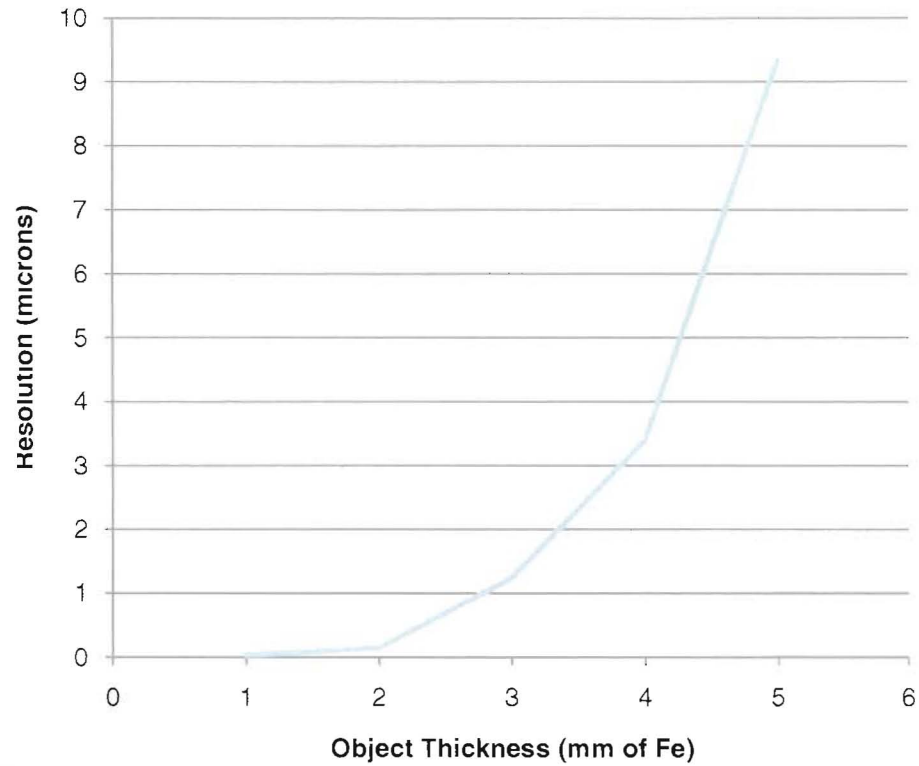

Long range tails are a problem.

Summary

- 800 MeV proton radiography continues to provide high quality dynamic materials studies for LANL.
- Gains in resolution have been realized through the development of magnifying lens systems.
- High energy proton radiography has been demonstrated at 24 GeV.
- Magnifying lens systems coupled with a high energy proton source could provide unprecedented views into dynamic systems.
  - 1% density measurements with micron resolution!
- Electrons may be a powerful probe for studying thin systems with high resolution.